A posteriori error analysis of mixed finite element methods for stress-assisted diffusion problems*

Gabriel N. Gatica† Bryan Gómez-Vargas‡ Ricardo Ruiz-Baier§

Abstract

We develop the a posteriori error analysis for mixed-primal and fully-mixed finite element methods approximating the stress-assisted diffusion of solutes in elastic materials. The systems are formulated in terms of stress, rotation and displacements for the elasticity equations, whereas the nonlinear diffusion is cast using either solute concentration (leading to a four-field mixed-primal formulation), or the triplet concentration - concentration gradient - and nonlinear diffusive flux (yielding the six-field fully-mixed variational formulation). We have addressed the well-posedness of these formulations in previous works, also introducing discretisations based on PEERS or Arnold-Falk-Winther elements for the linear elasticity and either Lagrange, or Lagrange - Raviart-Thomas - Lagrange triplets for the approximation of the diffusion equation. Here we advocate the derivation of two efficient and reliable residual-based a posteriori error estimators focusing on the two-dimensional case. The proofs of reliability depend on adequately formulated inf-sup conditions in combination with a Helmholtz decomposition, and they also rely on the local approximation features of Clément and Raviart-Thomas interpolations. The efficiency of the estimators results from classical inverse and discrete trace inequalities together with localisation techniques based on edge- and triangle-bubble functions. The theoretical properties of these error indicators are confirmed through numerical tests, also serving to illustrate the performance of the adaptive mesh refinement.

Key words: Linear elasticity, stress-assisted diffusion, mixed-primal formulation, fully-mixed formulation, finite element methods, a posteriori error analysis.

Mathematics subject classifications (2000): 65N30, 65N12, 65N15, 76R05, 76D07.

1 Introduction

The interaction of transport phenomena and chemical reactions within deformable media is a phenomenon encountered in a vast variety of scientific and engineering applications, including damage in lithium ion batteries [33], sorption in fibre-reinforced polymeric materials [32], diffusion of boron and arsenic in silicon [41], hydrogen diffusion in metals [34], anisotropy of cardiac dynamics [17],

*This work was partially supported by CONICYT-Chile through the project AFB170001 of the PIA Program: Concurso Apoyo a Centros Científicos y Tecnológicos de Excelencia con Financiamiento Basal, and the PhD fellowship for foreign students 21170275; by Centro de Investigación en Ingeniería Matemática (CI^{2}MA), Universidad de Concepción; and by the QJMAM Fund for Applied Mathematics 2019.

†CI^{2}MA and Departamento de Ingeniería Matemática, Universidad de Concepción, Casilla 160-C, Concepción, Chile, email: ggatica@ci2ma.udec.cl.

‡Sección de Matemática, Sede de Occidente, Universidad de Costa Rica, San Ramón, Costa Rica. Present address: CI^{2}MA and Departamento de Ingeniería Matemática, Universidad de Concepción, Casilla 160-C, Concepción, Chile, email: bgomez@ci2ma.udec.cl.

§Mathematical Institute, Oxford University, Andrew Wiles Building, Woodstock Road, OX2 6GG Oxford, UK, email: ruizbaier@maths.ox.ac.uk.

and several other effects. The modelling framework using continuum mechanics was developed in the early works [2, 36], and subsequently, a number of distinct models have been advanced [20, 33]. Mathematical analysis was provided in [29], while mixed formulations for these problems have been recently addressed in [25, 26], where we investigate steady systems where the main coupling variable is the Cauchy stress exerted by solid motion. In these works we have used a mixed form for elasticity in terms of stress, rotation and displacement. For the diffusion problem we have studied primal and mixed approaches: the first one in terms of the solute concentration, whereas the second one has been formulated in terms of diffusive flux, solute concentration and its gradient. We have invoked regularity estimates that only hold for the specific case of convex domains and in two spatial dimensions (see details on the assumptions and their implications in [25, Section 2.2]). We have also formulated the nonlinear set of equations as a fixed-point problem, analysing it using Schauder fixed-point theory and classical tools for saddle-point equations. The associated methods use PEERS and Arnold-Falk-Winther elements for the elasticity, and either Lagrange finite elements, or a triplet of Raviart-Thomas elements and piecewise polynomials for the primal and mixed forms of the diffusion equation, respectively.

It is well known that in order to rectify the convergence of numerical schemes in pathological situations (such as in presence of singularities in the solutions, in the data, or in the domain geometry), one can introduce mesh adaptation guided by a posteriori error estimators. These indicators are essentially global quantities $\boldsymbol{\Theta}$ that are expressed in terms of local estimators $\boldsymbol{\Theta}_K$ (fully computable as a function of the discrete solution and of the data) defined on each element of a given mesh. Then, $\boldsymbol{\Theta}$ is said to be efficient (resp. reliable) if there exists a constant $C_{\text{eff}} > 0$ (resp. C_{rel}), independent of the meshsize, such that $C_{\text{eff}}\boldsymbol{\Theta}+\text{h.o.t} \leq \|error\| \leq C_{\text{rel}}\boldsymbol{\Theta}+\text{h.o.t}$, where h.o.t contains high-order terms. Without knowing the exact solutions, these terms give an indication on which elements induce high errors (measured in a suitable norm) and should be considered for local refinement, thus guaranteeing that the discretisation error is controlled.

Diverse a posteriori error analyses for linear elasticity can be found in the literature, including for instance traditional primal schemes [14, 39], mixed finite element methods in stress-displacement-rotation form [13, 16, 30], augmented mixed approaches [11], pseudostress-based mixed formulations [24], mixed schemes with pure traction boundary conditions [21], using discontinuous Galerkin methods [40], or methods specifically tailored for incompressible materials [28], among others. In turn, a posteriori error analyses for elliptic equations have been widely investigated by many authors (see, e.g. [3, 37, 38] and the references therein). Although adaptive meshes are of key usefulness in computing solutions to stress-and-strain assisted diffusion of hydrogen in metals such as crack-capturing [34] and fatigue crack growth [35], a rigorous a posteriori error analysis specifically tailored for such coupled problems is still not available in the literature.

The lack of robustness of the two-way coupling between mechanical deformation and the chemical transport can affect the accuracy of the stress-assisted diffusion processes, especially under modelling peculiarities in either of the two problems. For instance, solutions with high gradients could lead to generating an excessive distortion of the finite element mesh. We therefore aim at developing robust and reliable a posteriori error estimators. Not many results are available for this particular type of problems, but we can draw inspiration from results where the elasticity and diffusion problems have been worked independently. Most of the a posteriori error estimators for elasticity in mixed form share similarities with those available for elliptic problems in divergence form, and therefore it is possible to establish an adequate analysis without the need of re-structuring the logical steps in the proofs of reliability and efficiency usually followed for classical approaches [4, 12, 13, 30, 31], as well as some more recent references concerning transport coupled with incompressible flow or related models, as in e.g. [5, 6, 7, 10, 15]. For the latter, one needs to carefully handle the coupling terms, invoking

properties of the nonlinear model functions (Lipschitz continuity, uniformly boundedness), as well as suitable regularity estimates.

The rest of this work is organised as follows. In Section 2 we introduce preliminary notation used throughout this work, and then we recall the model problem and establish some assumptions on data. The corresponding mixed-primal and fully-mixed variational formulations as well as their associated Galerkin schemes are presented in Section 3. Next, in Section 4, we derive the corresponding reliable and efficient residual-based a posteriori error indicators for our Galerkin schemes. Finally, in Section 5, our theoretical results are illustrated via some numerical examples, highlighting also the good performance of the associated adaptive schemes and properties of the proposed indicators.

2 The stress-assisted diffusion problem

2.1 Preliminary notation

Let us denote by $\Omega \subseteq \mathrm{R}^2$, a given convex domain with boundary $\Gamma = \partial\Omega$, and denote by $\boldsymbol{\nu}$ the outward unit normal vector on the boundary. We will adopt a fairly standard notation for Lebesgue and Sobolev spaces: $\mathrm{L}^p(\Omega)$ and $\mathrm{H}^s(\Omega)$, respectively. Norms and seminorms for the latter will be written as $\|\cdot\|_{s,\Omega}$ and $|\cdot|_{s,\Omega}$. The space $\mathrm{H}^{1/2}(\Gamma)$ contains traces of functions of $\mathrm{H}^1(\Omega)$, $\mathrm{H}^{-1/2}(\Gamma)$ denotes its dual, and $\langle\cdot,\cdot\rangle_\Gamma$ stands for the duality pairing between them. In general, the notation $\mathbf{M}$ and $\mathbb{M}$ will refer to vectorial and tensorial counterparts of a generic scalar functional space M. Furthermore, by

$$\|\boldsymbol{w}\|_{\infty,\Omega} := \max_{i=1,n}\{\|w_i\|_{\infty,\Omega}\}, \quad \text{and} \quad \|\psi\|_{1,\infty,\Omega} := \max_{\alpha\leq 1}\left(\operatorname*{ess\,sup}_{x\in\Omega}|\partial^\alpha\psi(x)|\right),$$

we will denote norms for the Banach spaces $\mathbf{L}^\infty(\Omega)$ and $\mathrm{W}^{1,\infty}(\Omega)$, respectively. Next we recall the definition of the tensorial Hilbert space and its usual norm

$$\mathbb{H}(\mathbf{div};\Omega) := \left\{\boldsymbol{\tau}\in\mathbb{L}^2(\Omega): \ \mathbf{div}\,\boldsymbol{\tau}\in\mathbf{L}^2(\Omega)\right\}, \quad \|\boldsymbol{\tau}\|^2_{\mathbf{div};\Omega} := \|\boldsymbol{\tau}\|^2_{0,\Omega} + \|\mathbf{div}\,\boldsymbol{\tau}\|^2_{0,\Omega},$$

where $\mathbf{div}\,\boldsymbol{\tau}$ indicates the divergence operator acting along the rows of the tensor field $\boldsymbol{\tau}$. As usual, $\mathbb{I}$ stands for the identity tensor in $\mathrm{R}^{2\times 2}$, and $|\cdot|$ denotes both the Euclidean norm in R^2 and the Frobenius norm in $\mathrm{R}^{2\times 2}$. Finally, for any tensor fields $\boldsymbol{\tau} = (\tau_{ij})_{i,j=1,2}$, and $\boldsymbol{\zeta} = (\zeta_{ij})_{i,j=1,2}$, we recall the transpose, trace, tensor product, and deviatoric splitting operators defined respectively as

$$\boldsymbol{\tau}^{\mathrm{t}} := (\tau_{ji})_{i,j=1,2}, \qquad \mathrm{tr}(\boldsymbol{\tau}) := \sum_{i=1}^{2}\tau_{ii} \qquad \boldsymbol{\tau}:\boldsymbol{\zeta} := \sum_{i,j=1}^{2}\tau_{ij}\zeta_{ij}, \qquad \text{and} \qquad \boldsymbol{\tau}^{\mathrm{d}} := \boldsymbol{\tau} - \frac{1}{2}\mathrm{tr}(\boldsymbol{\tau})\mathbb{I}.$$

2.2 Governing equations

Let us consider the following system of partial differential equations, governing the diffusion of a solute interacting with the motion of an elastic solid occupying the domain Ω:

$$\begin{array}{lllll} \boldsymbol{\sigma} = \lambda\,\mathrm{tr}\boldsymbol{\varepsilon}(\boldsymbol{u})\,\mathbb{I} + 2\mu\boldsymbol{\varepsilon}(\boldsymbol{u}) & \text{and} & -\,\mathbf{div}\,\boldsymbol{\sigma} = \boldsymbol{f}(\phi) \ \text{ in } \ \Omega, & \boldsymbol{u} = \boldsymbol{u}_{\mathrm{D}} & \text{on } \ \Gamma, \\ \widetilde{\boldsymbol{\sigma}} = \vartheta(\boldsymbol{\sigma})\nabla\phi & \text{and} & -\,\mathrm{div}\,\widetilde{\boldsymbol{\sigma}} = g(\boldsymbol{u}) \ \text{ in } \ \Omega, & \phi = 0 & \text{on } \ \Gamma, \end{array} \tag{2.1}$$

where ϕ represents the local concentration of species; $\boldsymbol{\sigma}$ is the Cauchy solid stress; $\boldsymbol{u}$ is the displacement field; $\boldsymbol{\varepsilon}(\boldsymbol{u}) := \frac{1}{2}\left(\nabla\boldsymbol{u} + \nabla\boldsymbol{u}^{\mathrm{t}}\right)$ is the infinitesimal strain tensor; $\widetilde{\boldsymbol{\sigma}}$ is the diffusive flux; $\lambda, \mu > 0$ are the Lamé constants; $\boldsymbol{u}_{\mathrm{D}} \in \mathbf{H}^{1/2}(\Gamma)$ is the corresponding Dirichlet condition for the displacement;

$\vartheta : \mathrm{R}^{2\times 2} \to \mathrm{R}^{2\times 2}$ is a tensorial diffusivity; $\boldsymbol{f} : \mathrm{R} \to \mathrm{R}^2$ is a vector field of body loads (which will depend on the species concentration), and $g : \mathrm{R}^2 \to \mathrm{R}$ denotes an additional source term depending locally on the solid displacement. In what follows we will suppose that ϑ is of class C^1, uniformly positive definite, uniformly bounded and Lipschitz continuous, meaning that there exist positive constants ϑ_0, ϑ_1, ϑ_2 and L_ϑ, such that

$$\begin{gathered} \vartheta(\boldsymbol{\tau})\boldsymbol{w}\cdot\boldsymbol{w} \geq \vartheta_0|\boldsymbol{w}|^2, \quad \vartheta_1 \leq |\vartheta(\boldsymbol{\tau})| \leq \vartheta_2 \quad \forall\, \boldsymbol{w} \in \mathrm{R}^2 \quad \forall\, \boldsymbol{\tau}, \boldsymbol{\zeta} \in \mathrm{R}^{2\times 2}, \\ |\vartheta(\boldsymbol{\tau}) - \vartheta(\boldsymbol{\zeta})| \leq L_\vartheta|\boldsymbol{\tau} - \boldsymbol{\zeta}| \quad \forall\, \boldsymbol{\tau}, \boldsymbol{\zeta} \in \mathrm{R}^{2\times 2}. \end{gathered} \tag{2.2}$$

Similar assumptions will be placed on the load and source functions $\boldsymbol{f}$ and g: we suppose that there exist positive constants f_1, f_2, L_f, g_1, g_2 and L_g, such that

$$f_1 \leq |\boldsymbol{f}(s)| \leq f_2, \quad |\boldsymbol{f}(s) - \boldsymbol{f}(t)| \leq L_f|s-t| \quad \forall\, s, t \in \mathrm{R}, \tag{2.3}$$

$$g_1 \leq g(\boldsymbol{w}) \leq g_2, \quad |g(\boldsymbol{v}) - g(\boldsymbol{w})| \leq L_g|\boldsymbol{v} - \boldsymbol{w}| \quad \forall\, \boldsymbol{v}, \boldsymbol{w} \in \mathrm{R}^2. \tag{2.4}$$

Moreover, for each $\gamma \in (0,1)$, there exists a constant $C_\gamma > 0$, such that $g(\boldsymbol{w}) \in \mathrm{H}^\gamma(\Omega)$ for each $\boldsymbol{w} \in \mathrm{H}^\gamma(\Omega)$, and

$$\|g(\boldsymbol{w})\|_{\gamma,\Omega} \leq C_\gamma \, \|\boldsymbol{w}\|_{\gamma,\Omega} \, .$$

Finally, we assume that for every $\phi \in \mathrm{H}^1(\Omega)$, we have $\boldsymbol{f}(\phi) \in \mathbf{H}^1(\Omega)$.

We point out that the reader may refer to [2, 17, 20, 25, 29] for further details concerning different variants of the model problem, as well as for specific examples of the nonlinear functions given above.

3 Continuous and discrete mixed formulations

In this section we recall the continuous and discrete mixed-primal and fully-mixed schemes for (2.1) derived in [25, Section 2] and [26, Section 3], respectively, and state their well-posedness.

3.1 Mixed-primal approach

The construction of a mixed formulation for the elasticity equation in (2.1) follows closely those in [23, 25]. Thus, from Hooke's law we have

$$\mathcal{C}^{-1}\boldsymbol{\sigma} = \boldsymbol{\varepsilon}(\boldsymbol{u}) = \nabla\boldsymbol{u} - \boldsymbol{\rho}, \quad \text{where} \quad \boldsymbol{\rho} := \frac{1}{2}(\nabla\boldsymbol{u} - \nabla\boldsymbol{u}^{\mathrm{t}}), \tag{3.1}$$

with $\boldsymbol{\rho} \in \mathbb{L}^2_{\mathrm{skew}}(\Omega) := \{\boldsymbol{\eta} \in \mathbb{L}^2(\Omega) : \quad \boldsymbol{\eta} + \boldsymbol{\eta}^{\mathrm{t}} = 0\}$. Moreover, an application of the orthogonal decomposition $\mathbb{H}(\mathbf{div};\Omega) = \mathbb{H}_0(\mathbf{div};\Omega) \oplus \mathrm{R}\mathbb{I}$, where

$$\mathbb{H}_0(\mathbf{div};\Omega) := \left\{ \boldsymbol{\tau} \in \mathbb{H}(\mathbf{div};\Omega) : \quad \int_\Omega \mathrm{tr}(\boldsymbol{\tau}) = 0 \right\},$$

allows us to only seek the $\mathbb{H}_0(\mathbf{div};\Omega)$-component of the stress, whereas the remaining unknows velocity and rotation are searched in $\mathbf{L}^2(\Omega)$ and $\mathbb{L}^2_{\mathrm{skew}}(\Omega)$, respectively. On the other hand, the boundary condition for ϕ indicates the appropriate trial and test space

$$\mathrm{H}^1_0(\Omega) := \left\{ \psi \in \mathrm{H}^1(\Omega) : \quad \psi = 0 \ \text{ on } \ \Gamma \right\},$$

to deduce the corresponding primal formulation for the diffusion equation (second row of (2.1)). Therefore, denoting from now on $\vec{\boldsymbol{\sigma}} := (\boldsymbol{\sigma}, \boldsymbol{u}, \boldsymbol{\rho}) \in \mathbf{H}_1 := \mathbb{H}_0(\mathbf{div}; \Omega) \times \mathbf{L}^2(\Omega) \times \mathbb{L}^2_{\mathrm{skew}}(\Omega)$, the mixed-primal variational formulation for our model problem (2.1) reads: Find $(\vec{\boldsymbol{\sigma}}, \phi) \in \mathbf{H}_1 \times \mathrm{H}^1_0(\Omega)$, such that

$$\begin{aligned} a(\boldsymbol{\sigma}, \boldsymbol{\tau}) + b(\boldsymbol{\tau}, (\boldsymbol{u}, \boldsymbol{\rho})) &= G(\boldsymbol{\tau}) && \forall\, \boldsymbol{\tau} \in \mathbb{H}_0(\mathbf{div}; \Omega), \\ b(\boldsymbol{\sigma}, (\boldsymbol{v}, \boldsymbol{\eta})) &= F_\phi(\boldsymbol{v}, \boldsymbol{\eta}) && \forall\, (\boldsymbol{v}, \boldsymbol{\eta}) \in \mathbf{L}^2(\Omega) \times \mathbb{L}^2_{\mathrm{skew}}(\Omega), \\ A_{\boldsymbol{\sigma}}(\phi, \psi) &= G_{\boldsymbol{u}}(\psi) && \forall\, \psi \in \mathrm{H}^1_0(\Omega), \end{aligned} \tag{3.2}$$

where the bilinear forms $a : \mathbb{H}_0(\mathbf{div}; \Omega) \times \mathbb{H}_0(\mathbf{div}; \Omega) \to \mathbb{R}$, $b : \mathbb{H}_0(\mathbf{div}; \Omega) \times (\mathbf{L}^2(\Omega) \times \mathbb{L}^2_{\mathrm{skew}}(\Omega)) \to \mathbb{R}$ and $A_{\boldsymbol{\sigma}} : \mathrm{H}^1_0(\Omega) \times \mathrm{H}^1_0(\Omega) \to \mathbb{R}$ are specified as

$$a(\boldsymbol{\zeta}, \boldsymbol{\tau}) := \int_\Omega \mathcal{C}^{-1}\boldsymbol{\sigma} : \boldsymbol{\tau} = \frac{1}{2\,\mu} \int_\Omega \boldsymbol{\zeta}^{\mathrm{d}} : \boldsymbol{\tau}^{\mathrm{d}} + \frac{1}{4(\lambda + \mu)} \int_\Omega \mathrm{tr}(\boldsymbol{\zeta})\, \mathrm{tr}(\boldsymbol{\tau}),$$

$$b(\boldsymbol{\tau}, (\boldsymbol{v}, \boldsymbol{\eta})) := \int_\Omega \boldsymbol{v} \cdot \mathbf{div}\, \boldsymbol{\tau} + \int_\Omega \boldsymbol{\eta} : \boldsymbol{\tau}, \qquad A_{\boldsymbol{\sigma}}(\varphi, \psi) := \int_\Omega \vartheta(\boldsymbol{\sigma}) \nabla\varphi \cdot \nabla\psi,$$

for $\boldsymbol{\zeta}, \boldsymbol{\tau} \in \mathbb{H}_0(\mathbf{div}; \Omega)$, $(\boldsymbol{v}, \boldsymbol{\eta}) \in \mathbf{L}^2(\Omega) \times \mathbb{L}^2_{\mathrm{skew}}(\Omega)$ and $\varphi, \psi \in \mathrm{H}^1_0(\Omega)$. In turn, the functionals $F_\phi \in (\mathbf{L}^2(\Omega) \times \mathbb{L}^2_{\mathrm{skew}}(\Omega))'$, $G \in \mathbb{H}_0(\mathbf{div}; \Omega)'$ and $G_{\boldsymbol{u}} \in \mathrm{H}^1_0(\Omega)'$ are given by

$$G(\boldsymbol{\tau}) := \langle \boldsymbol{\tau}\boldsymbol{\nu}, \boldsymbol{u}_{\mathrm{D}} \rangle_\Gamma, \quad F_\phi(\boldsymbol{v}, \boldsymbol{\eta}) := -\int_\Omega \boldsymbol{f}\,(\phi) \cdot \boldsymbol{v}, \qquad \text{and} \qquad G_{\boldsymbol{u}}(\psi) := \int_\Omega g(\boldsymbol{u})\, \psi\,,$$

for $\vec{\boldsymbol{\tau}} := (\boldsymbol{\tau}, \boldsymbol{v}, \boldsymbol{\eta}) \in \mathbf{H}_1$ and $\psi \in \mathrm{H}^1_0(\Omega)$. Further details yielding the weak formulation (3.2) can be found in [25, Section 2.1], whereas its solvability follows from the fixed-point strategy developed in [25, Theorem 2.9]. We point out that for future purposes and according to the new meaning of $\boldsymbol{\sigma}$, the constitutive equation (3.1) now becomes

$$\mathcal{C}^{-1}\boldsymbol{\sigma} + \boldsymbol{\rho} + \frac{1}{2|\Omega|} \left(\int_\Gamma \boldsymbol{u}_{\mathrm{D}} \cdot \boldsymbol{\nu} \right) \mathbb{I} = \nabla \boldsymbol{u} \qquad \text{in} \quad \Omega. \tag{3.3}$$

In view of defining a Galerkin formulation, let us denote by $\mathcal{T}_h$ a regular partition of $\overline{\Omega}$ into triangles K of diameter h_K, where $h := \max\{h_K : \ K \in \mathcal{T}_h\}$ is the meshsize. Given an integer $k \geq 0$, for each $K \in \mathcal{T}_h$ we let $\mathrm{P}_k(K)$ be the space of polynomial functions on K of degree $\leq k$ and define the local Raviart-Thomas space of order k as

$$\mathbf{RT}_k(K) := \mathbf{P}_k(K) \oplus \mathrm{P}_k(K)\, \boldsymbol{x},$$

where $\mathbf{P}_k(K) = [\mathrm{P}_k(K)]^2$, and $\boldsymbol{x}$ is a generic vector in R^2. Furthermore, using the above notation, we define the Brezzi-Douglas-Marini space $\mathbb{BDM}_{k+1}(K) := [\mathrm{P}_{k+1}(K)]^{2\times 2}$. Now, let b_K be the element bubble function defined as the unique polynomial in $\mathrm{P}_3(K)$ vanishing on ∂K with $\int_K b_K = 1$. Then, for each $K \in \mathcal{T}_h$ we consider the bubble space of order k, defined by

$$\mathbf{B}_k(K) := \mathrm{P}_k(K) \left(\frac{\partial b_K}{\partial x_2}, -\frac{\partial b_K}{\partial x_1} \right).$$

Now, denoting by $\vec{\boldsymbol{\sigma}}_h := (\boldsymbol{\sigma}_h, \boldsymbol{u}_h, \boldsymbol{\rho}_h) \in \mathbf{H}_{1,h} := \mathbb{H}^{\boldsymbol{\sigma}}_h \times \mathbf{H}^{\boldsymbol{u}}_h \times \mathbb{H}^{\boldsymbol{\rho}}_h$, the Galerkin scheme for (3.2) is defined as: find $(\vec{\boldsymbol{\sigma}}_h, \phi_h) \in \mathbf{H}_{1,h} \times \mathrm{H}^{\phi}_h$ such that

$$\begin{aligned} a(\boldsymbol{\sigma}_h, \boldsymbol{\tau}_h) + b(\boldsymbol{\tau}_h, (\boldsymbol{u}_h, \boldsymbol{\rho}_h)) &= G(\boldsymbol{\tau}_h) && \forall\, \boldsymbol{\tau}_h \in \mathbb{H}^{\boldsymbol{\sigma}}_h, \\ b(\boldsymbol{\sigma}_h, (\boldsymbol{v}_h, \boldsymbol{\eta}_h)) &= F_{\phi_h}(\boldsymbol{v}_h, \boldsymbol{\eta}_h) && \forall\, (\boldsymbol{v}_h, \boldsymbol{\eta}_h) \in \mathbf{H}^{\boldsymbol{u}}_h \times \mathbb{H}^{\boldsymbol{\rho}}_h, \\ A_{\boldsymbol{\sigma}_h}(\phi_h, \psi_h) &= G_{\boldsymbol{u}_h}(\psi_h) && \forall\, \psi_h \in \mathrm{H}^{\phi}_h, \end{aligned} \tag{3.4}$$

where the involved finite element spaces are defined similar to [25, 26]. Thus, for the elasticity equation we consider the classical PEERS elements [8]:

$$\begin{aligned}
\mathbb{H}_h^{\boldsymbol{\sigma}} &:= \left\{ \boldsymbol{\tau}_h \in \mathbb{H}_0(\mathbf{div};\Omega) : \quad \boldsymbol{\tau}_h|_K \in [\mathbf{RT}_k(K)]^2 \oplus [\mathbf{B}_k(K)]^2 \quad \forall\, K \in \mathcal{T}_h \right\}, \\
\mathbf{H}_h^{\boldsymbol{u}} &:= \left\{ \boldsymbol{v}_h \in \mathbf{L}^2(\Omega) : \quad \boldsymbol{v}_h|_K \in \mathbf{P}_k(K) \quad \forall\, K \in \mathcal{T}_h \right\}, \\
\mathbb{H}_h^{\boldsymbol{\rho}} &:= \left\{ \boldsymbol{\eta}_h \in \mathbb{L}^2_{\mathrm{skew}}(\Omega) : \quad \boldsymbol{\eta}_h \in \mathbf{C}(\overline{\Omega}) \quad \text{and} \quad \boldsymbol{\eta}_h|_K \in \mathbb{P}_{k+1}(K) \quad \forall\, K \in \mathcal{T}_h \right\},
\end{aligned} \tag{3.5}$$

and the Arnold-Falk-Winther elements [9]:

$$\begin{aligned}
\mathbb{H}_h^{\boldsymbol{\sigma}} &:= \left\{ \boldsymbol{\tau}_h \in \mathbb{H}_0(\mathbf{div};\Omega) : \quad \boldsymbol{\tau}_h|_K \in \mathbb{BDM}_{k+1}(K) \quad \forall\, K \in \mathcal{T}_h \right\}, \\
\mathbf{H}_h^{\boldsymbol{u}} &:= \left\{ \boldsymbol{v}_h \in \mathbf{L}^2(\Omega) : \quad \boldsymbol{v}_h|_K \in \mathbf{P}_k(K) \quad \forall\, K \in \mathcal{T}_h \right\}, \\
\mathbb{H}_h^{\boldsymbol{\rho}} &:= \left\{ \boldsymbol{\eta}_h \in \mathbb{L}^2_{\mathrm{skew}}(\Omega) : \quad \boldsymbol{\eta}_h|_K \in \mathbb{P}_k(K) \quad \forall\, K \in \mathcal{T}_h \right\},
\end{aligned} \tag{3.6}$$

whereas the approximating space for the concentration is defined as

$$\mathrm{H}_h^{\phi} := \left\{ \psi_h \in \mathrm{C}(\overline{\Omega}) \cap \mathrm{H}_0^1(\Omega) \quad \psi_h|_K \in \mathrm{P}_{k+1}(K) \quad \forall\, K \in \mathcal{T}_h \right\}.$$

The solvability and a priori error bounds for (3.2) and (3.4) are established in [25, Sections 2-3]. Denoting by c_p the Poincaré constant and defining the balls

$$W := \left\{ \phi \in \mathrm{H}_0^1(\Omega) : \ \|\phi\|_{1,\Omega} \leq \frac{c_p^2}{\vartheta_0} g_2 |\Omega|^{1/2} \right\} \quad \text{and} \quad W_h := \left\{ \phi_h \in \mathrm{H}_h^{\phi} : \ \|\phi_h\|_{1,\Omega} \leq \frac{c_p^2}{\vartheta_0} g_2 |\Omega|^{1/2} \right\},$$

we will assume through the rest of the paper that $(\vec{\boldsymbol{\sigma}}, \phi) \in \mathbf{H}_1 \times \mathrm{H}_0^1(\Omega)$ with $\phi \in W$, and $(\vec{\boldsymbol{\sigma}}_h, \phi_h) \in \mathbf{H}_{1,h} \times \mathrm{H}_h^{\phi}$ with $\phi_h \in W_h$, are the solutions of the continuous and discrete formulations (3.2) and (3.4), respectively. In addition, we recall from [25, Theorems 2.9 and 3.7] the following a priori estimates

$$\|\vec{\boldsymbol{\sigma}}\|_{\mathbf{H}_1} \leq c_{\mathbf{S}} \left\{ \|\boldsymbol{u}_{\mathrm{D}}\|_{1/2,\Gamma} + f_2 |\Omega|^{1/2} \right\}, \qquad \|\vec{\boldsymbol{\sigma}}_h\|_{\mathbf{H}_1} \leq \widetilde{C} \left\{ \|\boldsymbol{u}_{\mathrm{D}}\|_{1/2,\Gamma} + f_2 |\Omega|^{1/2} \right\},$$

where $c_{\mathbf{S}}$ and $\widetilde{C}$ are positive constants independent of ϕ and ϕ_h.

3.2 Fully-mixed approach

Having established in Section 3.1 the mixed formulation for the elasticity problem, it only remains to define a mixed formulation for the diffusion equation. Proceeding as in [26], we define $\boldsymbol{t} := \nabla\phi$, and consider the following Galerkin type terms:

$$\begin{aligned}
\kappa_1 \int_\Omega \{\widetilde{\boldsymbol{\sigma}} - \vartheta(\boldsymbol{\sigma})\, \boldsymbol{t}\} \cdot \widetilde{\boldsymbol{\tau}} = 0 \qquad & \forall\, \widetilde{\boldsymbol{\tau}} \in \mathbf{H}(\mathrm{div};\Omega), \\
\kappa_2 \int_\Omega \mathrm{div}\, \widetilde{\boldsymbol{\sigma}}\, \mathrm{div}\, \widetilde{\boldsymbol{\tau}} = -\kappa_2 \int_\Omega g(\boldsymbol{u})\, \mathrm{div}\, \widetilde{\boldsymbol{\tau}} \qquad & \forall\, \widetilde{\boldsymbol{\tau}} \in \mathbf{H}(\mathrm{div};\Omega), \\
\kappa_3 \int_\Omega \{\nabla\phi - \boldsymbol{t}\} \cdot \nabla\psi = 0 \qquad & \forall\, \psi \in \mathrm{H}_0^1(\Omega),
\end{aligned}$$

where κ_1, κ_2 and κ_3 are positive parameters to be suitably chosen. Let us group appropriately the unknowns and spaces of the diffusion problem as follows: $\widetilde{\underline{\boldsymbol{\sigma}}} := (\widetilde{\boldsymbol{\sigma}}, \boldsymbol{t}, \phi) \in \mathbf{H}_2 := \mathbf{H}(\mathrm{div};\Omega) \times \mathbf{L}^2(\Omega) \times \mathrm{H}_0^1(\Omega)$. We then have an augmented formulation for the diffusion problem: find $\widetilde{\underline{\boldsymbol{\sigma}}} \in \mathbf{H}_2$ such that

$$A_{\boldsymbol{\sigma}}(\widetilde{\underline{\boldsymbol{\sigma}}}, \widetilde{\underline{\boldsymbol{\tau}}}) = G_{\boldsymbol{u}}(\widetilde{\underline{\boldsymbol{\tau}}}) \quad \forall\, \widetilde{\underline{\boldsymbol{\tau}}} := (\widetilde{\boldsymbol{\tau}}, \boldsymbol{s}, \psi) \in \mathbf{H}_2,$$

where

$$A_{\boldsymbol{\sigma}}(\widetilde{\underline{\boldsymbol{\sigma}}},\widetilde{\underline{\boldsymbol{\tau}}}) := \int_\Omega \vartheta(\boldsymbol{\sigma})\,\boldsymbol{t}\cdot\boldsymbol{s} - \int_\Omega \widetilde{\boldsymbol{\sigma}}\cdot\boldsymbol{s} + \int_\Omega \widetilde{\boldsymbol{\tau}}\cdot\boldsymbol{t} + \int_\Omega \phi\,\mathrm{div}\,\widetilde{\boldsymbol{\tau}} - \int_\Omega \psi\,\mathrm{div}\,\widetilde{\boldsymbol{\sigma}}$$
$$+\ \kappa_1\int_\Omega \{\widetilde{\boldsymbol{\sigma}} - \vartheta(\boldsymbol{\sigma})\,\boldsymbol{t}\}\cdot\widetilde{\boldsymbol{\tau}} + \kappa_2\int_\Omega \mathrm{div}\,\widetilde{\boldsymbol{\sigma}}\,\mathrm{div}\,\widetilde{\boldsymbol{\tau}} + \kappa_3\int_\Omega \{\nabla\phi - \boldsymbol{t}\}\cdot\nabla\psi,$$
$$G_{\boldsymbol{u}}(\widetilde{\underline{\boldsymbol{\tau}}}) := \int_\Omega \psi\,g(\boldsymbol{u}) - \kappa_2\int_\Omega g(\boldsymbol{u})\,\mathrm{div}\,\widetilde{\boldsymbol{\tau}}.$$

Consequently, we arrive at the following augmented fully-mixed formulation to system (2.1): find $(\vec{\boldsymbol{\sigma}},\widetilde{\underline{\boldsymbol{\sigma}}}) \in \mathbf{H}_1\times\mathbf{H}_2$, such that

$$\begin{array}{rcll} a(\boldsymbol{\sigma},\boldsymbol{\tau}) + b(\boldsymbol{\tau},(\boldsymbol{u},\boldsymbol{\rho})) & = & G(\boldsymbol{\tau}) & \forall\,\boldsymbol{\tau}\in\mathbb{H}_0(\mathbf{div};\Omega), \\ b(\boldsymbol{\sigma},(\boldsymbol{v},\boldsymbol{\eta})) & = & F_\phi(\boldsymbol{v},\boldsymbol{\eta}) & \forall\,(\boldsymbol{v},\boldsymbol{\eta})\in\mathbf{L}^2(\Omega)\times\mathbb{L}^2_{\mathrm{skew}}(\Omega), \\ A_{\boldsymbol{\sigma}}(\widetilde{\underline{\boldsymbol{\sigma}}},\widetilde{\underline{\boldsymbol{\tau}}}) & = & G_{\boldsymbol{u}}(\widetilde{\underline{\boldsymbol{\tau}}}) & \forall\,\widetilde{\underline{\boldsymbol{\tau}}}\in\mathbf{H}_2. \end{array} \tag{3.7}$$

In turn, denoting from now on $\widetilde{\underline{\boldsymbol{\sigma}}}_h := (\widetilde{\boldsymbol{\sigma}}_h,\boldsymbol{t}_h,\phi_h)\in\mathbf{H}_{2,h} := \mathbf{H}_h^{\widetilde{\boldsymbol{\sigma}}}\times\mathbf{H}_h^{\boldsymbol{t}}\times\mathrm{H}_h^{\phi}$, the associated Galerkin scheme reads: find $(\vec{\boldsymbol{\sigma}}_h,\widetilde{\underline{\boldsymbol{\sigma}}}_h)\in\mathbf{H}_{1,h}\times\mathbf{H}_{2,h}$ such that

$$\begin{array}{rl} a(\boldsymbol{\sigma}_h,\boldsymbol{\tau}_h) + b(\boldsymbol{\tau}_h,(\boldsymbol{u}_h,\boldsymbol{\rho}_h)) = G(\boldsymbol{\tau}_h) & \forall\,\boldsymbol{\tau}_h\in\mathbb{H}_h^{\boldsymbol{\sigma}}, \\ b(\boldsymbol{\sigma}_h,(\boldsymbol{v}_h,\boldsymbol{\eta}_h)) = F_{\phi_h}(\boldsymbol{v}_h,\boldsymbol{\eta}_h) & \forall\,(\boldsymbol{v}_h,\boldsymbol{\eta}_h)\in\mathbf{H}_h^{\boldsymbol{u}}\times\mathbb{H}_h^{\boldsymbol{\rho}}, \\ A_{\boldsymbol{\sigma}_h}(\widetilde{\underline{\boldsymbol{\sigma}}}_h,\widetilde{\underline{\boldsymbol{\tau}}}_h) = G_{\boldsymbol{u}_h}(\widetilde{\underline{\boldsymbol{\tau}}}_h) & \forall\,\widetilde{\underline{\boldsymbol{\tau}}}_h := (\widetilde{\boldsymbol{\tau}}_h,\boldsymbol{s}_h,\psi_h)\in\mathbf{H}_{2,h}, \end{array} \tag{3.8}$$

where $\mathbf{H}_{1,h}$ is as in Section 3.1, and the remaining spaces are:

$$\begin{array}{l} \mathbf{H}_h^{\widetilde{\boldsymbol{\sigma}}} := \{\widetilde{\boldsymbol{\tau}}_h\in\mathbf{H}(\mathrm{div};\Omega):\quad \widetilde{\boldsymbol{\tau}}_h|_K\in\mathbf{RT}_k(K)\quad\forall\,K\in\mathcal{T}_h\}, \\ \mathbf{H}_h^{\boldsymbol{t}} := \{\boldsymbol{t}_h\in\mathbf{L}^2(\Omega):\quad \boldsymbol{t}_h|_K\in\mathbf{P}_k(K)\quad\forall\,K\in\mathcal{T}_h\}, \\ \mathrm{H}_h^{\phi} := \{\psi_h\in\mathrm{C}(\overline{\Omega})\cap\mathrm{H}_0^1(\Omega):\quad \psi_h|_K\in\mathrm{P}_{k+1}(K)\quad\forall\,K\in\mathcal{T}_h\}. \end{array} \tag{3.9}$$

Finally, similarly as in Section 3.1, and defining the balls

$$W := \left\{\phi\in\mathrm{H}_0^1(\Omega):\ \ \|\phi\|_{1,\Omega}\le\widetilde{c}_{\mathbf{S}}g_2|\Omega|^{1/2}\right\}\quad\text{and}\quad W_h := \left\{\phi_h\in\mathrm{H}_h^{\phi}:\ \ \|\phi_h\|_{1,\Omega}\le\widetilde{c}_{\mathbf{S}}g_2|\Omega|^{1/2}\right\},$$

where $\widetilde{c}_{\mathbf{S}}$ is a constant depending only on data and other constants, we let $(\vec{\boldsymbol{\sigma}},\widetilde{\underline{\boldsymbol{\sigma}}})\in\mathbf{H}_1\times\mathbf{H}_2$ with $\phi\in W$, and $(\vec{\boldsymbol{\sigma}}_h,\widetilde{\underline{\boldsymbol{\sigma}}}_h)\in\mathbf{H}_{1,h}\times\mathbf{H}_{2,h}$ with $\phi_h\in W_h$, be the solutions of the continuous and discrete formulations (3.7) and (3.8), respectively. Additionally, we recall from [26, Theorems 3.9 and 4.7] that the following a priori estimates hold

$$\|\widetilde{\underline{\boldsymbol{\sigma}}}\|_{\mathbf{H}_2}\le\widetilde{c}_{\mathbf{S}}g_2|\Omega|^{1/2},\qquad \|\vec{\boldsymbol{\sigma}}\|_{\mathbf{H}_1}\le c_{\mathbf{S}}\left\{\|\boldsymbol{u}_{\mathrm{D}}\|_{1/2,\Gamma}+f_2|\Omega|^{1/2}\right\},$$
$$\|\widetilde{\underline{\boldsymbol{\sigma}}}_h\|_{\mathbf{H}_2}\le\widetilde{c}_{\mathbf{S}}g_2|\Omega|^{1/2},\qquad \|\vec{\boldsymbol{\sigma}}_h\|_{\mathbf{H}_1}\le\widetilde{C}\left\{\|\boldsymbol{u}_{\mathrm{D}}\|_{1/2,\Gamma}+f_2|\Omega|^{1/2}\right\}.$$

4 Residual-based a posteriori error estimators

The main goal of this section is to derive reliable and efficient residual-based a posteriori error estimators for the Galerkin schemes (3.4) and (3.8).

4.1 Preliminaries

Further notation is needed for describing local information on elements and edges. Given $K \in \mathcal{T}_h$, we let $\mathcal{E}_h(K)$ be the set of its edges, and let $\mathcal{E}_h$ be the set of all edges of the triangulation $\mathcal{T}_h$, whose corresponding diameters are denoted by h_e. Then, we write $\mathcal{E}_h = \mathcal{E}_h(\Omega) \cup \mathcal{E}_h(\Gamma)$, where $\mathcal{E}_h(\Omega) := \{e \in \mathcal{E}_h : e \subseteq \Omega\}$ and $\mathcal{E}_h(\Gamma) := \{e \in \mathcal{E}_h : e \subseteq \Gamma\}$. Also, for each edge e of $\mathcal{E}_h$ we fix a unit normal and tangential vectors $\boldsymbol{\nu}$ and $\boldsymbol{s}$ to e. Thus, the usual jump operator $[\![\cdot]\!]$ across an internal edge $e \in \mathcal{E}_h(\Omega)$ is defined for piecewise continuous tensor, vector, or scalar-valued functions $\boldsymbol{\zeta}$ as

$$[\![\boldsymbol{\zeta}]\!] = \boldsymbol{\zeta}|_{K_+} - \boldsymbol{\zeta}|_{K_-} ,$$

where K_- and K_+ are the triangles of $\mathcal{T}_h$ sharing the edge e. Additionally, given scalar, vector and tensor fields φ, $\boldsymbol{\varphi} := (\varphi_1, \varphi_2)$ and $\boldsymbol{\tau} := (\tau_{ij})$, respectively, we set

$$\mathbf{rot}(\varphi) := \begin{pmatrix} \frac{\partial \varphi}{\partial x_2} \\ -\frac{\partial \varphi}{\partial x_1} \end{pmatrix}, \quad \mathrm{rot}(\boldsymbol{\varphi}) := \frac{\partial \varphi_2}{\partial x_1} - \frac{\partial \varphi_1}{\partial x_2},$$

$$\underline{\mathbf{curl}}(\boldsymbol{\varphi}) := \begin{pmatrix} \frac{\partial \varphi_1}{\partial x_2} & -\frac{\partial \varphi_1}{\partial x_1} \\ \frac{\partial \varphi_2}{\partial x_2} & -\frac{\partial \varphi_2}{\partial x_1} \end{pmatrix}, \quad \text{and} \quad \mathbf{curl}(\boldsymbol{\tau}) := \begin{pmatrix} \frac{\partial \tau_{12}}{\partial x_1} - \frac{\partial \tau_{11}}{\partial x_2} \\ \frac{\partial \tau_{22}}{\partial x_1} - \frac{\partial \tau_{21}}{\partial x_2} \end{pmatrix}.$$

Next, we collect a few preliminary definitions and results that we need in what follows. We begin by recalling the usual Clément interpolation operator (cf. [19]) $\mathrm{I}_h : \mathrm{H}^1(\Omega) \to \mathrm{X}_h$, where

$$\mathrm{X}_h := \left\{ \varphi_h \in \mathrm{C}(\overline{\Omega}) : \quad \varphi_h|_K \in \mathrm{P}_1(K) \quad \forall\, K \in \mathcal{T}_h \right\}.$$

A vectorial version of I_h, say $\mathbf{I}_h : \mathbf{H}^1(\Omega) \to \mathbf{X}_h := \mathrm{X}_h \times \mathrm{X}_h$, which is defined component-wise by I_h, will be needed as well. Moreover, to satisfy homogeneous Dirichlet boundary conditions, we introduce the Clément-type interpolation operator $\widetilde{\mathrm{I}}_h : \mathrm{H}^1_0(\Omega) \to \widetilde{\mathrm{X}}_h$, where

$$\widetilde{\mathrm{X}}_h := \left\{ \varphi_h \in \mathrm{C}(\overline{\Omega}) \cap \mathrm{H}^1_0(\Omega) : \quad \varphi_h|_K \in \mathrm{P}_1(K) \quad \forall\, K \in \mathcal{T}_h \right\}.$$

The following lemma provides the local approximation properties of I_h (for a proof, see [19]). Analogue estimates hold for the operators $\mathbf{I}_h$ and $\widetilde{\mathrm{I}}_h$.

Lemma 4.1 *There exist $c_1, c_2 > 0$, independent of h, such that for each $\varphi \in \mathrm{H}^1(\Omega)$, there holds*

$$\|\varphi - \mathrm{I}_h(\varphi)\|_{0,K} \leq c_1 h_K \, |\varphi|_{1,\Delta(K)} \quad \forall\, K \in \mathcal{T}_h, \tag{4.1}$$

and

$$\|\varphi - \mathrm{I}_h(\varphi)\|_{0,e} \leq c_2 h_e^{1/2} \, |\varphi|_{1,\Delta(e)} \quad \forall\, e \in \mathcal{E}_h, \tag{4.2}$$

where $\Delta(K) := \cup\{K' \in \mathcal{T}_h : \quad K' \cap K \neq 0\}$ and $\Delta(e) := \cup\{K' \in \mathcal{T}_h : \quad K' \cap e \neq 0\}$.

Moreover, we also introduce the usual Raviart-Thomas interpolator $\Pi_h : \mathbf{H}^1(\Omega) \to \mathbf{H}_h^{\widetilde{\boldsymbol{\sigma}}}$ [23, Section 3.4.1], which, given $\boldsymbol{\tau} \in \mathbf{H}^1(\Omega)$, is characterised by

$$\int_e \Pi_h(\boldsymbol{\tau}) \cdot \boldsymbol{\nu} \Psi = \int_e \boldsymbol{\tau} \cdot \boldsymbol{\nu} \Psi, \qquad \forall \, \text{edge } e \in \mathcal{T}_h, \ \forall\, \Psi \in \mathrm{P}_k(e), \tag{4.3}$$

$$\int_K \Pi_h(\boldsymbol{\tau}) \cdot \boldsymbol{\xi} = \int_K \boldsymbol{\tau} \cdot \boldsymbol{\xi} \quad \forall\, K \in \mathcal{T}_h, \qquad \forall\, \boldsymbol{\xi} \in \mathbf{P}_{k-1}(K), \ \text{ when } k \geq 1. \tag{4.4}$$

Additionally, using (4.3) and (4.4), the commuting diagram property yields

$$\mathrm{div}(\Pi_h(\boldsymbol{\tau})) = \mathcal{P}_h(\mathrm{div}\,\boldsymbol{\tau}) \quad \forall\, \boldsymbol{\tau} \in \mathbf{H}^1(\Omega), \tag{4.5}$$

where $\mathcal{P}_h$ is the $\mathrm{L}^2(\Omega)$-orthogonal projector onto the space of piecewise scalar polynomials of degree $\leq k$. Further approximations properties of Π_h are summarised in the following lemma (see a proof in e.g [23, Lemmas 3.16 and 3.18]).

Lemma 4.2 *There exist $C_1, C_2 > 0$, independent of h, such that for all $\boldsymbol{\tau} \in \mathbf{H}^1(\Omega)$, there hold*

$$\|\boldsymbol{\tau} - \Pi_h(\boldsymbol{\tau})\|_{0,K} \leq C_1 h_K \, \|\boldsymbol{\tau}\|_{1,K} \quad \forall\, K \in \mathcal{T}_h, \tag{4.6}$$

$$\|(\boldsymbol{\tau} - \Pi_h(\boldsymbol{\tau}))\boldsymbol{\nu}\|_{0,e} \leq C_2 h_e^{1/2} \, \|\boldsymbol{\tau}\|_{1,K_e} \quad \forall\, e \in \mathcal{E}_h, \tag{4.7}$$

where K_e in (4.7) is a triangle of $\mathcal{T}_h$ containing the edge e on its boundary.

A tensor version of Π_h, say $\boldsymbol{\Pi}_h : \mathbb{H}^1(\Omega) \to \mathbb{RT}_k$, (where $\mathbb{RT}_k$ is the space of pure Raviart-Thomas tensors of order k), which is defined row-wise by Π_h, and a vector version of $\mathcal{P}_h$, say, $\boldsymbol{\mathcal{P}}_h$ which is the $\mathbf{L}^2(\Omega)$-orthogonal projector onto $\mathbf{H}_h^{\boldsymbol{u}}$ (cf. (3.5), (3.6)), that is the space of piecewise vector valued polynomials of degree $\leq k$, might also be required. For simplicity of the presentation we have focused on the Raviart-Thomas interpolator. However, if we would like to use the family (3.6), we might use the BDM interpolator, which also satisfies the approximation properties given above.

In addition, we recall a Helmholtz decomposition of $\mathbb{H}_0(\mathbf{div};\Omega)$, which will be essential in the subsequent analysis. We refer to [27, Lemma 3.7] for further details.

Lemma 4.3 *For each $\boldsymbol{\tau} \in \mathbb{H}_0(\mathbf{div};\Omega)$, there exist $\boldsymbol{z} \in \mathbf{H}^2(\Omega)$ and $\boldsymbol{\Phi} \in \mathbf{H}^1(\Omega)$, such that*

$$\boldsymbol{\tau} = \nabla \boldsymbol{z} + \underline{\mathbf{curl}}\, \boldsymbol{\Phi} \ \text{ in } \ \Omega, \quad \text{and} \quad \|\boldsymbol{z}\|_{2,\Omega} + \|\boldsymbol{\Phi}\|_{1,\Omega} \leq C \, \|\boldsymbol{\tau}\|_{\mathbf{div};\Omega}\,. \tag{4.8}$$

On the other hand, the main techniques involved below in the proof of efficiency include the localisation technique based on element-bubble and edge-bubble functions. In view of this, we let ψ_e and ψ_K be the usual edge-bubble and face-bubble functions (see [38]), respectively, which satisfy $\psi_e|_K \in \mathrm{P}_2(K)$, $\mathrm{supp}\,\psi_e \subseteq \omega_e := \cup\{K' \in \mathcal{T}_h : e \in \mathcal{E}_h(K')\}, \psi_e = 0$ on $\partial K \backslash e$ and $0 \leq \psi_e \leq 1$ in ω_e, and $\psi_K \in \mathrm{P}_3(K)$, $\mathrm{supp}\,\psi_K \subseteq K, \psi_K = 0$ on ∂K and $0 \leq \psi_K \leq 1$ in K, respectively. We also recall from [37] that, given $k \in \mathbb{N} \cup \{0\}$, there exists an extension operator $\mathrm{L} : C(e) \to C(K)$ satisfying $\mathrm{L}(p) \in \mathrm{P}_k(K)$ and $\mathrm{L}(p)|_e = p \ \ \forall\, p \in \mathrm{P}_k(e)$. A corresponding vector version of L, that is the component-wise application of L, is denote by $\mathbf{L}$. Additional properties of ψ_e, ψ_K and L are collected in the following lemma (see e.g. [38]).

Lemma 4.4 *Given $k \in \mathbb{N} \cup \{0\}$, there exist positive constants c_3, c_4 and c_5, depending only on k, and the shape regularity of the triangulations (minimum angle condition), such that for each $K \in \mathcal{T}_h$ and $e \in \mathcal{E}_h(K)$, there hold*

$$\|q\|_{0,K}^2 \leq c_3 \|\psi_K^{1/2} q\|_{0,K}^2 \quad \forall\, q \in \mathrm{P}_k(K), \tag{4.9}$$

$$\|p\|_{0,e}^2 \leq c_4 \|\psi_e^{1/2} p\|_{0,e}^2 \quad \forall\, p \in \mathrm{P}_k(e), \tag{4.10}$$

$$\|\psi_e \, \mathrm{L}(p)\|_{0,K}^2 \leq \|\psi_e^{1/2} \, \mathrm{L}(p)\|_{0,K}^2 \leq c_5 \, h_e \, \|p\|_{0,e}^2 \quad \forall\, p \in \mathrm{P}_k(e). \tag{4.11}$$

Furthermore, we will also need the following inverse estimate (cf. [18, Theorem 3.2.6]) and discrete trace inequality (cf. [1, Theorem 3.10]), respectively.

Lemma 4.5 *Let k, l, $m \in \mathbb{N} \cup \{0\}$ such that $l \leq m$. Then, there exists $c_6 > 0$, depending only on k, l, m and the shape regularity of the triangulations, such that for each $K \in \mathcal{T}_h$, there holds*

$$|q|_{m,K} \leq c_6 \, h_K^{l-m} |q|_{l,K} \quad \forall \, q \in \mathrm{P}_k(K).$$

Lemma 4.6 *There exists $c_7 > 0$, depending only on the shape regularity of the triangulations, such that for each $K \in \mathcal{T}_h$ and $e \in \mathcal{E}_h(K)$, there holds*

$$\|v\|_{0,e}^2 \leq c_7 \left\{ h_e^{-1} \, \|v\|_{0,K}^2 + h_e |v|_{1,K}^2 \right\} \quad \forall \, v \in \mathrm{H}^1(K). \tag{4.12}$$

Finally, the following lemma is applied next to the terms involving the **curl** and **rot** operators, and the tangential jumps across the edges of $\mathcal{T}_h$. Its proof, which makes use of Lemmas 4.4 and 4.6, can be found in [11, Lemmas 4.3 and 4.4].

Lemma 4.7 *Let $\boldsymbol{\xi}_h \in \mathbb{L}^2(\Omega)$ be a piecewise polynomial tensor of degree $k \geq 0$ on each $K \in \mathcal{T}_h$, and let $\boldsymbol{\xi} \in \mathbb{L}^2(\Omega)$ be such that $\mathbf{curl}(\boldsymbol{\xi}) = \mathbf{0}$ in Ω. Then, there exist $c_8, c_9 > 0$, independent of h, such that*

$$\|\mathbf{curl}(\boldsymbol{\xi}_h)\|_{0,K} \leq c_8 \, h_K^{-1} \, \|\boldsymbol{\xi} - \boldsymbol{\xi}_h\|_{0,K} \quad \forall \, K \in \mathcal{T}_h,$$
$$\|[\![\boldsymbol{\xi}_h \boldsymbol{s}]\!]\|_{0,e} \leq c_9 \, h_e^{-1/2} \, \|\boldsymbol{\xi} - \boldsymbol{\xi}_h\|_{0,\omega_e} \quad \forall \, e \in \mathcal{E}_h(\Omega).$$

4.2 A posteriori error analysis for the mixed-primal scheme

In this section we derive a reliable and efficient residual-based a posteriori error estimator for (3.4). We begin by defining for each $K \in \mathcal{T}_h$ the local error indicator $\boldsymbol{\Theta}_K := \boldsymbol{\Theta}_{E,K} + \boldsymbol{\Theta}_{D,K}$, where $\boldsymbol{\Theta}_{E,K}$ and $\boldsymbol{\Theta}_{D,K}$ are the corresponding quantities associated with the elasticity and diffusion equations, respectively, which are given by:

$$\begin{aligned}
\boldsymbol{\Theta}_{E,K}^2 := {} & \|\boldsymbol{f}(\phi_h) + \mathbf{div}\, \boldsymbol{\sigma}_h\|_{0,K}^2 + \|\boldsymbol{\sigma}_h - \boldsymbol{\sigma}_h^{\mathrm{t}}\|_{0,K}^2 + h_K^2 \left\| \nabla \boldsymbol{u}_h - \left(\mathcal{C}^{-1} \boldsymbol{\sigma}_h + \boldsymbol{\rho}_h + c\mathbb{I} \right) \right\|_{0,K}^2 \\
& + h_K^2 \left\| \mathbf{curl} \left(\mathcal{C}^{-1} \boldsymbol{\sigma}_h + \boldsymbol{\rho}_h \right) \right\|_{0,K}^2 + \sum_{e \in \mathcal{E}_h(\Omega) \cap \mathcal{E}_h(K)} h_e \left\| [\![(\mathcal{C}^{-1} \boldsymbol{\sigma}_h + \boldsymbol{\rho}_h + c\mathbb{I}) \boldsymbol{s}]\!] \right\|_{0,e}^2 \\
& + \sum_{e \in \mathcal{E}_h(\Gamma) \cap \mathcal{E}_h(K)} h_e \left\{ \left\| \frac{d \boldsymbol{u}_{\mathrm{D}}}{d \boldsymbol{s}} - (\mathcal{C}^{-1} \boldsymbol{\sigma}_h + \boldsymbol{\rho}_h + c\mathbb{I}) \boldsymbol{s} \right\|_{0,e}^2 + \|\boldsymbol{u}_{\mathrm{D}} - \boldsymbol{u}_h\|_{0,e}^2 \right\},
\end{aligned} \tag{4.13}$$

and

$$\boldsymbol{\Theta}_{D,K}^2 := h_K^2 \, \|\mathrm{div} \left(\vartheta(\boldsymbol{\sigma}_h) \nabla \phi_h \right) + g(\boldsymbol{u}_h)\|_{0,K}^2 + \sum_{e \in \mathcal{E}_h(\Omega) \cap \mathcal{E}_h(K)} h_e \, \|[\![\vartheta(\boldsymbol{\sigma}_h) \nabla \phi_h \cdot \boldsymbol{\nu}]\!]\|_{0,e}^2 \,, \tag{4.14}$$

where

$$c := \frac{1}{2|\Omega|} \int_\Gamma \boldsymbol{u}_{\mathrm{D}} \cdot \boldsymbol{\nu}. \tag{4.15}$$

We remark in advance that the above requires that $\frac{d \boldsymbol{u}_{\mathrm{D}}}{d \boldsymbol{s}} \in \mathbf{L}^2(e)$ for each $e \in \mathcal{E}_h(\Gamma)$. This is fixed below assuming that $\boldsymbol{u}_{\mathrm{D}} \in \mathbf{H}^1(\Gamma)$. Finally, we point out that the residual character of each term defining $\boldsymbol{\Theta}_{E,K}$, $\boldsymbol{\Theta}_{D,K}$, and hence $\boldsymbol{\Theta}_K$, is clear, and then, proceeding as usual, the global residual estimator can be defined as:

$$\boldsymbol{\Theta} := \left\{ \sum_{K \in \mathcal{T}_h} \boldsymbol{\Theta}_K^2 \right\}^{1/2}.$$

The remainder of this section advocates to show the existence of positive constants $C_{\rm eff}$ and $C_{\rm rel}$, independent of the meshsizes and the continuous and discrete solutions, such that

$$C_{\rm eff}\boldsymbol{\Theta} \leq \|(\vec{\boldsymbol{\sigma}},\phi)-(\vec{\boldsymbol{\sigma}}_h,\phi_h)\| \leq C_{\rm rel}\boldsymbol{\Theta}. \tag{4.16}$$

The efficiency of the global a posteriori error estimator (lower bound in (4.16)) is proved below in Section 4.2.2, whereas the corresponding reliability (upper bound in (4.16)) is derived in Section 4.2.1.

In order to establish the reliability of the a posteriori error estimator $\boldsymbol{\Theta}$, we apply the global inf-sup condition and the uniform ellipticity of some bilinear forms, together with smallness-of-data assumptions.

We begin with a preliminary estimate for the partial elasticity error $\|\vec{\boldsymbol{\sigma}}-\vec{\boldsymbol{\sigma}}_h\|_{\mathbf{H}_1}$.

Lemma 4.8 *There exists $C_1>0$, independent of λ and h, such that*

$$\begin{aligned}\|\vec{\boldsymbol{\sigma}}-\vec{\boldsymbol{\sigma}}_h\|_{\mathbf{H}_1} \leq C_1 \Big\{ &\|\mathcal{R}^E\|_{\mathbb{H}_0(\mathbf{div};\Omega)'} + L_f\,\|\phi-\phi_h\|_{1,\Omega} \\ &+ \|f(\phi_h)+\mathbf{div}\,\boldsymbol{\sigma}_h\|_{0,\Omega} + \|\boldsymbol{\sigma}_h-\boldsymbol{\sigma}_h^{\rm t}\|_{0,\Omega}\Big\},\end{aligned} \tag{4.17}$$

where the functional $\mathcal{R}^E$ is defined by

$$\mathcal{R}^E(\boldsymbol{\tau}) := G(\boldsymbol{\tau}) - a(\boldsymbol{\sigma}_h,\boldsymbol{\tau}) - b(\boldsymbol{\tau},(\boldsymbol{u}_h,\boldsymbol{\rho}_h)) \quad \forall\,\boldsymbol{\tau}\in\mathbb{H}_0(\mathbf{div};\Omega). \tag{4.18}$$

Furthermore, there holds

$$\mathcal{R}^E(\boldsymbol{\tau}_h)=0 \quad \forall\,\boldsymbol{\tau}_h\in\mathbb{H}_h^{\boldsymbol{\sigma}}. \tag{4.19}$$

Proof. We begin the derivation of (4.17) by recalling from [23, Section 2.4.3.1], that b satisfies the inf-sup condition and that a is elliptic in the kernel of b. Then, there exists $C>0$, independent of h, such that for each $\vec{\boldsymbol{\xi}} := (\boldsymbol{\xi},\boldsymbol{w},\boldsymbol{\zeta})\in\mathbf{H}_1$, the following global inf-sup condition holds (see [22, Proposition 2.36])

$$C\|\vec{\boldsymbol{\xi}}\|_{\mathbf{H}_1} \leq \sup_{\substack{\vec{\boldsymbol{\tau}}\in\mathbf{H}_1\\ \vec{\boldsymbol{\tau}}\neq\mathbf{0}}} \frac{a(\boldsymbol{\xi},\boldsymbol{\tau})+b(\boldsymbol{\tau},(\boldsymbol{w},\boldsymbol{\zeta}))+b(\boldsymbol{\xi},(\boldsymbol{v},\boldsymbol{\eta}))}{\|\vec{\boldsymbol{\tau}}\|_{\mathbf{H}_1}}.$$

In particular, for the error $\vec{\boldsymbol{\xi}} := \vec{\boldsymbol{\sigma}}-\vec{\boldsymbol{\sigma}}_h$, using the notation introduced by (4.18), and applying some algebraic manipulations, we have

$$\begin{aligned}C\|\vec{\boldsymbol{\sigma}}-\vec{\boldsymbol{\sigma}}_h\|_{\mathbf{H}_1} &\leq \sup_{\substack{\vec{\boldsymbol{\tau}}\in\mathbf{H}_1\\ \vec{\boldsymbol{\tau}}\neq\mathbf{0}}} \frac{a(\boldsymbol{\sigma}-\boldsymbol{\sigma}_h,\boldsymbol{\tau})+b(\boldsymbol{\tau},(\boldsymbol{u}-\boldsymbol{u}_h,\boldsymbol{\rho}-\boldsymbol{\rho}_h))+b(\boldsymbol{\sigma}-\boldsymbol{\sigma}_h,(\boldsymbol{v},\boldsymbol{\eta}))}{\|\vec{\boldsymbol{\tau}}\|_{\mathbf{H}_1}} \\ &\leq \sup_{\substack{\boldsymbol{\tau}\in\mathbb{H}_0(\mathbf{div};\Omega)\\ \boldsymbol{\tau}\neq\mathbf{0}}} \frac{|\mathcal{R}^E(\boldsymbol{\tau})|}{\|\boldsymbol{\tau}\|} + \sup_{\substack{(\boldsymbol{v},\boldsymbol{\eta})\in\mathbf{L}^2(\Omega)\times\mathbb{L}^2_{\rm skew}(\Omega)\\ (\boldsymbol{v},\boldsymbol{\eta})\neq\mathbf{0}}} \frac{|b(\boldsymbol{\sigma}-\boldsymbol{\sigma}_h,(\boldsymbol{v},\boldsymbol{\eta}))|}{\|(\boldsymbol{v},\boldsymbol{\eta})\|}.\end{aligned} \tag{4.20}$$

Now, according to the definition of the bilinear form b, adding and subtracting suitable terms, and then, applying the Lipschitz continuity of $\boldsymbol{f}$ (cf. (2.3)), the Cauchy-Schwarz inequality, and the fact that $\int_\Omega \boldsymbol{\sigma}_h : \boldsymbol{\eta} = \frac{1}{2}\int_\Omega (\boldsymbol{\sigma}_h-\boldsymbol{\sigma}_h^{\rm t}) : \boldsymbol{\eta}$, we get for all $(\boldsymbol{v},\boldsymbol{\eta})\in\mathbf{L}^2(\Omega)\times\mathbb{L}^2_{\rm skew}(\Omega)$

$$|b(\boldsymbol{\sigma}-\boldsymbol{\sigma}_h,(\boldsymbol{v},\boldsymbol{\eta}))| \leq \widetilde{C}\Big\{L_f\,\|\phi-\phi_h\|_{1,\Omega} + \|f(\phi_h)+\mathbf{div}\,\boldsymbol{\sigma}_h\|_{0,\Omega} + \|\boldsymbol{\sigma}_h-\boldsymbol{\sigma}_h^{\rm t}\|_{0,\Omega}\Big\}\,\|(\boldsymbol{v},\boldsymbol{\eta})\|\,,$$

which, together with (4.20), yields (4.17). Finally, it is readily seen that (4.19) follows directly from the first row of (3.4) and (4.18). □

We now derive an analogous preliminary bound for the error associated with $\|\phi-\phi_h\|_{1,\Omega}$.

Lemma 4.9 *There exists $C_2 > 0$, independent of h, such that*

$$\begin{aligned}\|\phi - \phi_h\|_{1,\Omega} \leq C_2 \Big\{ &\|\mathcal{R}^D\|_{\mathrm{H}_0^1(\Omega)'} + L_\vartheta \, c_{\mathbf{S}} \left(\|\boldsymbol{u}_{\mathrm{D}}\|_{1/2,\Gamma} + f_2 |\Omega|^{1/2} \right) \|\boldsymbol{\sigma} - \boldsymbol{\sigma}_h\|_{\mathbf{div};\Omega} \\ &+ \vartheta_2 \, \|\phi - \phi_h\|_{1,\Omega} + L_g \, \|\boldsymbol{u} - \boldsymbol{u}_h\|_{0,\Omega} \Big\} ,\end{aligned} \tag{4.21}$$

where the functional $\mathcal{R}^D$ is defined by

$$\mathcal{R}^D(\psi) := G_{\boldsymbol{u}_h}(\psi) \; - \; A_{\boldsymbol{\sigma}_h}(\phi_h, \psi) \quad \forall \, \psi \in \mathrm{H}_0^1(\Omega). \tag{4.22}$$

Furthermore, there holds

$$\mathcal{R}^D(\psi_h) = 0 \quad \forall \, \psi_h \in \mathrm{H}_h^\phi. \tag{4.23}$$

Proof. Similarly to the proof of Lemma 4.8, we first observe from the $\mathrm{H}_0^1(\Omega)$-ellipticity of $A_{\boldsymbol{\sigma}}$ (cf. [25, Lemma 2.3]) that the global inf-sup condition holds

$$\alpha \, \|\varphi\|_{1,\Omega} \leq \sup_{\substack{\psi \in \mathrm{H}_0^1(\Omega) \\ \psi \neq 0}} \frac{A_{\boldsymbol{\sigma}}(\varphi, \psi)}{\|\psi\|_{1,\Omega}} \quad \forall \, \varphi \in \mathrm{H}_0^1(\Omega), \tag{4.24}$$

where α is the ellipticity constant of $A_{\boldsymbol{\sigma}}$ [25, eq. (2.18)]. Then, applying (4.24) to the error $\varphi := \phi - \phi_h$, bearing in mind the definition (4.22), and adding and subtracting suitable terms, we find that

$$\alpha \, \|\phi - \phi_h\|_{1,\Omega} \leq \sup_{\substack{\psi \in \mathrm{H}_0^1(\Omega) \\ \psi \neq 0}} \frac{\mathcal{R}^D(\psi) + A_{\boldsymbol{\sigma}_h}(\phi_h, \psi) - A_{\boldsymbol{\sigma}}(\phi_h, \psi) + G_{\boldsymbol{u}}(\psi) - G_{\boldsymbol{u}_h}(\psi)}{\|\psi\|_{1,\Omega}}. \tag{4.25}$$

Now, recalling from [25, Section 2] that there exists a constant $C_\infty > 0$, such that the following estimate for the solution of the diffusion problem $\phi \in \mathrm{H}_0^1(\Omega)$ holds

$$\|\phi\|_{1,\infty,\Omega} \leq C_\infty \, c_{\mathbf{S}} \left(\|\boldsymbol{u}_{\mathrm{D}}\|_{1/2,\Gamma} + f_2 |\Omega|^{1/2} \right) ,$$

we can deduce the following result

$$\begin{aligned} &|A_{\boldsymbol{\sigma}_h}(\phi_h, \psi) - A_{\boldsymbol{\sigma}}(\phi_h, \psi)| \\ &\quad \leq \Big\{ \|\phi\|_{1,\infty,\Omega} \, L_\vartheta \, \|\boldsymbol{\sigma} - \boldsymbol{\sigma}_h\|_{\mathbf{div};\Omega} + 2\vartheta_2 \, \|\phi - \phi_h\|_{1,\Omega} \Big\} \, \|\psi\|_{1,\Omega} , \\ &\quad \leq \Big\{ C_\infty \, L_\vartheta c_{\mathbf{S}} \left(\|\boldsymbol{u}_{\mathrm{D}}\|_{1/2,\Gamma} + f_2 |\Omega|^{1/2} \right) \|\boldsymbol{\sigma} - \boldsymbol{\sigma}_h\|_{\mathbf{div};\Omega} + 2\vartheta_2 \, \|\phi - \phi_h\|_{1,\Omega} \Big\} \, \|\psi\|_{1,\Omega} . \end{aligned} \tag{4.26}$$

Moreover, applying the Lipschitz continuity of g (cf. (2.4)), we get

$$|G_{\boldsymbol{u}}(\psi) - G_{\boldsymbol{u}_h}(\psi)| \leq L_g \, \|\boldsymbol{u} - \boldsymbol{u}_h\|_{0,\Omega} \, \|\psi\|_{0,\Omega} . \tag{4.27}$$

Thus, replacing (4.26) and (4.27) back into (4.25) we obtain (4.21). Finally, using the fact that $G_{\boldsymbol{u}_h}(\psi_h) - A_{\boldsymbol{\sigma}_h}(\phi_h, \psi_h) = 0 \quad \forall \, \psi_h \in \mathrm{H}_h^\phi$, we get (4.23) and the proof concludes. □

Consequently, we can establish the following preliminary upper bound for the total error.

Theorem 4.10 *Assume that*

$$C_1 L_f + C_2 \left\{ \, \|\boldsymbol{u}_{\mathrm{D}}\|_{1/2,\Gamma} + f_2 |\Omega|^{1/2} + \vartheta_2 + L_g \right\} < \frac{1}{2}. \tag{4.28}$$

Then, there exists $C_3 > 0$, independent of λ and h, such that the total error satisfies

$$\begin{aligned} &\|(\vec{\boldsymbol{\sigma}}, \phi) - (\vec{\boldsymbol{\sigma}}_h, \phi_h)\| \\ &\qquad \leq C_3 \left\{ \|\mathcal{R}^E\|_{\mathbb{H}_0(\mathbf{div};\Omega)'} + \|f(\phi_h) + \mathbf{div}\, \boldsymbol{\sigma}_h\|_{0,\Omega} + \|\boldsymbol{\sigma}_h - \boldsymbol{\sigma}_h^{\mathrm{t}}\|_{0,\Omega} + \|\mathcal{R}^D\|_{\mathrm{H}_0^1(\Omega)'} \right\} . \end{aligned} \tag{4.29}$$

Proof. It follows as a straightforward application of (4.28) and Lemmas 4.8 and 4.9. □

It is clear from (4.29) that, in order to obtain an explicit estimate for the total error, it only remains to derive suitable upper bounds for $\|\mathcal{R}^E\|_{\mathbb{H}_0(\mathbf{div};\Omega)'}$ and $\|\mathcal{R}^D\|_{\mathrm{H}^1_0(\Omega)'}$. This is precisely the purpose of the next subsection.

4.2.1 Reliability

With the aim of estimating $\|\mathcal{R}^E\|_{\mathbb{H}_0(\mathbf{div};\Omega)'}$ we now take an arbitrary $\boldsymbol{\tau} \in \mathbb{H}_0(\mathbf{div};\Omega)$ and consider the Helmholtz decomposition provided by (4.8) (cf. Lemma 4.3). Then, we denote $\boldsymbol{\Phi}_h := \mathbf{I}_h(\boldsymbol{\Phi})$ and define $\boldsymbol{\tau}_h := \boldsymbol{\Pi}_h(\nabla \boldsymbol{z}) + \underline{\mathbf{curl}}(\boldsymbol{\Phi}_h) - d_h\,\mathbb{I} \in \mathbb{R}\mathbb{T}_k$, with $\boldsymbol{\Pi}_h$ the interpolator operator defined in Section 4.1, and where according to [24, Section 4.1], the constant d_h, which is defined by

$$d_h := -\frac{1}{2|\Omega|}\int_\Omega \mathrm{tr}(\nabla \boldsymbol{z} - \boldsymbol{\Pi}_h(\nabla \boldsymbol{z}) + \underline{\mathbf{curl}}(\boldsymbol{\Phi} - \boldsymbol{\Phi}_h)), \tag{4.30}$$

is chosen so that $\boldsymbol{\tau}_h$ belongs to $\mathbb{H}^{\boldsymbol{\sigma}}_h$ (cf. (3.5)). It follows that $\boldsymbol{\tau} - \boldsymbol{\tau}_h = \nabla \boldsymbol{z} - \boldsymbol{\Pi}_h(\nabla \boldsymbol{z}) + \underline{\mathbf{curl}}(\boldsymbol{\Phi} - \boldsymbol{\Phi}_h) + d_h\,\mathbb{I}$, and then, applying the tensor version of (4.5), we get

$$\mathbf{div}(\boldsymbol{\tau} - \boldsymbol{\tau}_h) = \mathbf{div}\big(\nabla \boldsymbol{z} - \boldsymbol{\Pi}_h(\nabla \boldsymbol{z})\big) = (\mathbb{I} - \boldsymbol{\mathcal{P}}_h)(\mathbf{div}\,\nabla \boldsymbol{z}) = (\mathbb{I} - \boldsymbol{\mathcal{P}}_h)(\mathbf{div}\,\boldsymbol{\tau}),$$

which is $\mathbf{L}^2(\Omega)$-orthogonal to $\mathbf{H}^{\boldsymbol{u}}_h$, and hence,

$$\int_\Omega \boldsymbol{u}_h \cdot \mathbf{div}(\boldsymbol{\tau} - \boldsymbol{\tau}_h) = \int_\Omega \boldsymbol{u}_h \cdot (\mathbb{I} - \boldsymbol{\mathcal{P}}_h)(\mathbf{div}\,\boldsymbol{\tau}) = 0. \tag{4.31}$$

Furthermore, taking into account that $\boldsymbol{\sigma}_h \in \mathbb{H}^{\boldsymbol{\sigma}}_h$ and $\boldsymbol{\rho}_h \in \mathbb{H}^{\boldsymbol{\rho}}_h$, and recalling that c and d_h are given by (4.15) and (4.30), respectively, we deduce from the definition of $\mathcal{R}^E$ (cf. (4.18)) that

$$\begin{aligned}\mathcal{R}^E(d_h\mathbb{I}) &= d_h\int_\Gamma \boldsymbol{u}_{\mathrm{D}}\cdot\boldsymbol{\nu} = -c\int_\Omega \mathrm{tr}\big(\nabla \boldsymbol{z} - \boldsymbol{\Pi}_h(\nabla \boldsymbol{z}) + \underline{\mathbf{curl}}(\boldsymbol{\Phi} - \boldsymbol{\Phi}_h)\big)\\ &= -\int_\Omega c\mathbb{I}\colon\big(\nabla \boldsymbol{z} - \boldsymbol{\Pi}_h(\nabla \boldsymbol{z})\big) - \int_\Omega c\mathbb{I}\colon \underline{\mathbf{curl}}(\boldsymbol{\Phi} - \boldsymbol{\Phi}_h),\end{aligned} \tag{4.32}$$

where for the second row in (4.32) we have applied the equality $\mathrm{tr}(\boldsymbol{\xi}) = \boldsymbol{\xi}\colon\mathbb{I}$. Thus, applying the null property (4.19), we find that

$$\mathcal{R}^E(\boldsymbol{\tau}) = \mathcal{R}^E(\boldsymbol{\tau} - \boldsymbol{\tau}_h) = \mathcal{R}^E\big(\nabla \boldsymbol{z} - \boldsymbol{\Pi}_h(\nabla \boldsymbol{z})\big) + \mathcal{R}^E\big(\underline{\mathbf{curl}}(\boldsymbol{\Phi} - \boldsymbol{\Phi}_h)\big) + \mathcal{R}^E(d_h\mathbb{I}),$$

from which, replacing the last adding by (4.32), recalling the definition of $\mathcal{R}^E$ (cf. (4.18)), and employing the identity (4.31), we deduce that $\mathcal{R}^E(\boldsymbol{\tau})$ can be decomposed as

$$\mathcal{R}^E(\boldsymbol{\tau}) = \mathcal{R}^E(\boldsymbol{\tau} - \boldsymbol{\tau}_h) = \mathcal{R}^E_1(\boldsymbol{z}) + \mathcal{R}^E_2(\boldsymbol{\Phi}) \qquad \forall\,\boldsymbol{\tau} \in \mathbb{H}_0(\mathbf{div};\Omega)\,, \tag{4.33}$$

where

$$\begin{aligned}\mathcal{R}^E_1(\boldsymbol{z}) &:= \mathcal{R}^E\big(\nabla \boldsymbol{z} - \boldsymbol{\Pi}_h(\nabla \boldsymbol{z})\big) - \int_\Omega c\mathbb{I}\colon\big(\nabla \boldsymbol{z} - \boldsymbol{\Pi}_h(\nabla \boldsymbol{z})\big)\\ &= \langle\big(\nabla \boldsymbol{z} - \boldsymbol{\Pi}_h(\nabla \boldsymbol{z})\big)\boldsymbol{\nu}, \boldsymbol{u}_{\mathrm{D}}\rangle_\Gamma - \int_\Omega (\mathcal{C}^{-1}\boldsymbol{\sigma}_h + \boldsymbol{\rho}_h + c\mathbb{I})\colon\big(\nabla \boldsymbol{z} - \boldsymbol{\Pi}_h(\nabla \boldsymbol{z})\big),\end{aligned} \tag{4.34}$$

and

$$\begin{aligned}\mathcal{R}^E_2(\boldsymbol{\Phi}) &:= \mathcal{R}^E(\underline{\mathbf{curl}}(\boldsymbol{\Phi} - \boldsymbol{\Phi}_h)) - \int_\Omega c\mathbb{I}\colon \underline{\mathbf{curl}}(\boldsymbol{\Phi} - \boldsymbol{\Phi}_h)\\ &= \langle\underline{\mathbf{curl}}(\boldsymbol{\Phi} - \boldsymbol{\Phi}_h)\boldsymbol{\nu}, \boldsymbol{u}_{\mathrm{D}}\rangle_\Gamma - \int_\Omega (\mathcal{C}^{-1}\boldsymbol{\sigma}_h + \boldsymbol{\rho}_h + c\mathbb{I})\colon \underline{\mathbf{curl}}(\boldsymbol{\Phi} - \boldsymbol{\Phi}_h).\end{aligned} \tag{4.35}$$

The following two lemmas provide upper bounds for (4.34) and (4.35).

Lemma 4.11 *There exists $C_4 > 0$, independent of λ and h, such that*

$$|\mathcal{R}_1^E(\boldsymbol{z})| \leq C_4 \left\{ \sum_{K \in \mathcal{T}_h} h_K^2 \left\| \nabla \boldsymbol{u}_h - \left(\mathcal{C}^{-1} \boldsymbol{\sigma}_h + \boldsymbol{\rho}_h + c\mathbb{I} \right) \right\|_{0,K}^2 + \sum_{e \in \mathcal{E}_h(\Gamma)} h_e \left\| \boldsymbol{u}_{\mathrm{D}} - \boldsymbol{u}_h \right\|_{0,e}^2 \right\}^{1/2} \left\| \boldsymbol{\tau} \right\|_{\mathbf{div};\Omega} .$$

Proof. It follows from an application of the tensor version of properties (4.3) and (4.4) to $\boldsymbol{u}_h|_e \in \mathbf{P}_k(e)$ for each $e \in \mathcal{E}_h$ and $\nabla \boldsymbol{u}_h|_K \in \mathbf{P}_{k-1}(K)$ for each $K \in \mathcal{T}_h$, respectively, and approximation results (4.6) and (4.7), in conjunction with the continuous dependence given by the Helmholtz decomposition (cf. (4.8)). We omit further details and refer to [24, Lemma 4.4]. □

Lemma 4.12 *If $\boldsymbol{u}_{\mathrm{D}} \in \mathbf{H}^1(\Gamma)$, then there exists $C_5 > 0$, independent of λ and h, such that*

$$\begin{aligned} |\mathcal{R}_2^E(\boldsymbol{\Phi})| \leq C_5 \left\{ \sum_{K \in \mathcal{T}_h} h_K^2 \left\| \mathbf{curl}(\mathcal{C}^{-1} \boldsymbol{\sigma}_h + \boldsymbol{\rho}_h) \right\|_{0,K}^2 + \sum_{e \in \mathcal{E}_h(\Omega)} h_e \left\| [\![(\mathcal{C}^{-1} \boldsymbol{\sigma}_h + \boldsymbol{\rho}_h + c\mathbb{I}) \boldsymbol{s}]\!] \right\|_{0,e}^2 \right. \\ \left. + \sum_{e \in \mathcal{E}_h(\Gamma)} h_e \left\| \frac{d \boldsymbol{u}_{\mathrm{D}}}{d \boldsymbol{s}} - (\mathcal{C}^{-1} \boldsymbol{\sigma}_h + \boldsymbol{\rho}_h + c\mathbb{I}) \boldsymbol{s} \right\|_{0,e}^2 \right\}^{1/2} \left\| \boldsymbol{\tau} \right\|_{\mathbf{div};\Omega} . \end{aligned} \tag{4.36}$$

Proof. We begin by applying the result given by [27, Lemma 3.8], to obtain

$$\langle \underline{\mathbf{curl}} \, (\boldsymbol{\Phi} - \boldsymbol{\Phi}_h) \boldsymbol{\nu}, \boldsymbol{u}_{\mathrm{D}} \rangle_\Gamma = - \left\langle \frac{d \boldsymbol{u}_{\mathrm{D}}}{d \boldsymbol{s}}, \boldsymbol{\Phi} - \boldsymbol{\Phi}_h \right\rangle_\Gamma = - \sum_{e \in \mathcal{E}_h(\Gamma)} \int_e (\boldsymbol{\Phi} - \boldsymbol{\Phi}_h) \, \frac{d \boldsymbol{u}_{\mathrm{D}}}{d \boldsymbol{s}} . \tag{4.37}$$

In turn, integrating by parts the second term on the right-hand side of (4.35), we get

$$\begin{aligned} \int_\Omega (\mathcal{C}^{-1} \boldsymbol{\sigma}_h + \boldsymbol{\rho}_h + c\mathbb{I}) : \underline{\mathbf{curl}} (\boldsymbol{\Phi} - \boldsymbol{\Phi}_h) = \sum_{K \in \mathcal{T}_h} \int_K \mathbf{curl}(\mathcal{C}^{-1} \boldsymbol{\sigma}_h + \boldsymbol{\rho}_h + c\mathbb{I}) \cdot (\boldsymbol{\Phi} - \boldsymbol{\Phi}_h) \\ - \sum_{e \in \mathcal{E}_h(\Omega)} \int_e [\![(\mathcal{C}^{-1} \boldsymbol{\sigma}_h + \boldsymbol{\rho}_h + c\mathbb{I}) \boldsymbol{s}]\!] \cdot (\boldsymbol{\Phi} - \boldsymbol{\Phi}_h) - \sum_{e \in \mathcal{E}_h(\Gamma)} \int_e (\mathcal{C}^{-1} \boldsymbol{\sigma}_h + \boldsymbol{\rho}_h + c\mathbb{I}) \boldsymbol{s} \cdot (\boldsymbol{\Phi} - \boldsymbol{\Phi}_h), \end{aligned}$$

which together with (4.37) yields

$$\begin{aligned} & \langle \underline{\mathbf{curl}} (\boldsymbol{\Phi} - \boldsymbol{\Phi}_h) \boldsymbol{\nu}, \boldsymbol{u}_{\mathrm{D}} \rangle_\Gamma - \int_\Omega (\mathcal{C}^{-1} \boldsymbol{\sigma}_h + \boldsymbol{\rho}_h + c\mathbb{I}) : \underline{\mathbf{curl}} (\boldsymbol{\Phi} - \boldsymbol{\Phi}_h) \\ & = - \sum_{K \in \mathcal{T}_h} \int_K \mathbf{curl}(\mathcal{C}^{-1} \boldsymbol{\sigma}_h + \boldsymbol{\rho}_h + c\mathbb{I}) \cdot (\boldsymbol{\Phi} - \boldsymbol{\Phi}_h) + \sum_{e \in \mathcal{E}_h(\Omega)} \int_e [\![(\mathcal{C}^{-1} \boldsymbol{\sigma}_h + \boldsymbol{\rho}_h + c\mathbb{I}) \boldsymbol{s}]\!] \cdot (\boldsymbol{\Phi} - \boldsymbol{\Phi}_h) \\ & \quad - \sum_{e \in \mathcal{E}_h(\Gamma)} \int_e \left\{ \frac{d \boldsymbol{u}_{\mathrm{D}}}{d \boldsymbol{s}} - (\mathcal{C}^{-1} \boldsymbol{\sigma}_h + \boldsymbol{\rho}_h + c\mathbb{I}) \boldsymbol{s} \right\} \cdot (\boldsymbol{\Phi} - \boldsymbol{\Phi}_h). \end{aligned}$$

Finally, employing the Cauchy-Schwarz inequality, the vector version of estimates (4.1) and (4.2), the fact that $\Delta(K)$ and $\Delta(e)$ are bounded, and the continuous dependence (4.8), we obtain (4.36). □

With the above two results, and bearing in mind the decomposition (4.33), we are in a position to complete an upper bound for $\|\mathcal{R}^E\|_{\mathbb{H}_0(\mathbf{div};\Omega)'}$.

Lemma 4.13 *Assume that $\boldsymbol{u}_{\mathrm{D}} \in \mathbf{H}^1(\Gamma)$. Then, there exists $\widehat{C}_1 > 0$, independent of λ and h, such that*

$$\|\mathcal{R}^E\|_{\mathbb{H}_0(\mathbf{div};\Omega)'} \leq \widehat{C}_1 \left\{ \sum_{K\in\mathcal{T}_h} h_K^2 \left\|\nabla \boldsymbol{u}_h - \left(\mathcal{C}^{-1}\boldsymbol{\sigma}_h + \boldsymbol{\rho}_h + c\mathbb{I}\right)\right\|_{0,K}^2 + \sum_{K\in\mathcal{T}_h} h_K^2 \left\|\mathbf{curl}(\mathcal{C}^{-1}\boldsymbol{\sigma}_h + \boldsymbol{\rho}_h)\right\|_{0,K}^2 \right.$$
$$+ \sum_{e\in\mathcal{E}_h(\Gamma)} h_e \left(\left\| \frac{d\boldsymbol{u}_{\mathrm{D}}}{d\boldsymbol{s}} - (\mathcal{C}^{-1}\boldsymbol{\sigma}_h + \boldsymbol{\rho}_h + c\mathbb{I})\boldsymbol{s} \right\|_{0,e}^2 + \|\boldsymbol{u}_{\mathrm{D}} - \boldsymbol{u}_h\|_{0,e}^2 \right)$$
$$\left. + \sum_{e\in\mathcal{E}_h(\Omega)} h_e \left\|[\![(\mathcal{C}^{-1}\boldsymbol{\sigma}_h + \boldsymbol{\rho}_h + c\mathbb{I})\boldsymbol{s}]\!]\right\|_{0,e}^2 \right\}^{1/2} .$$

In turn, we now provide an upper bound for $\|\mathcal{R}^D\|_{\mathrm{H}_0^1(\Omega)'}$.

Lemma 4.14 *There exists a constant $\widehat{C}_2 > 0$, independent of h, such that*

$$\|\mathcal{R}^D\|_{\mathrm{H}_0^1(\Omega)'} \leq \widehat{C}_2 \left\{ \sum_{K\in\mathcal{T}_h} h_K^2 \left\|\mathrm{div}\left(\vartheta(\boldsymbol{\sigma}_h)\nabla\phi_h\right) + g(\boldsymbol{u}_h)\right\|_{0,K}^2 \right.$$
$$\left. + \sum_{e\in\mathcal{E}_h(\Omega)} h_e \left\|[\![\vartheta(\boldsymbol{\sigma}_h)\nabla\phi_h \cdot \boldsymbol{\nu}]\!]\right\|_{0,e}^2 \right\}^{1/2} . \tag{4.38}$$

Proof. Given $\psi \in \mathrm{H}_0^1(\Omega)$, we let $\Psi_h := \widetilde{\mathrm{I}}_h(\psi) \in \mathrm{H}_h^\phi$. Thus, recalling the null property (4.23), the definition of the involved residual (cf. (4.22)), and integrating by parts, we obtain

$$\mathcal{R}^D(\psi - \Psi_h) = \int_\Omega g(\boldsymbol{u}_h)(\psi - \Psi_h) - \int_\Omega \vartheta(\boldsymbol{\sigma}_h)\nabla\phi_h \cdot \nabla(\psi - \Psi_h)$$
$$= \sum_{K\in\mathcal{T}_h} \int_K \left\{ g(\boldsymbol{u}_h) + \mathrm{div}\left(\vartheta(\boldsymbol{\sigma}_h)\nabla\phi_h\right)\right\}(\psi - \Psi_h) - \sum_{e\in\mathcal{E}_h(\Omega)} \int_e [\![\vartheta(\boldsymbol{\sigma}_h)\nabla\phi_h \cdot \boldsymbol{\nu}]\!](\psi - \Psi_h).$$

Finally, applying the Cauchy-Schwarz inequality and the estimates given by Lemma 4.1, we deduce the estimate

$$|\mathcal{R}^D(\psi - \Psi_h)| \leq \widehat{C}_2 \left\{ \sum_{K\in\mathcal{T}_h} h_K^2 \left\|g(\boldsymbol{u}_h) + \mathrm{div}\left(\vartheta(\boldsymbol{\sigma}_h)\nabla\phi_h\right)\right\|_{0,K}^2 \right.$$
$$\left. + \sum_{e\in\mathcal{E}_h(\Omega)} h_e \left\|[\![\vartheta(\boldsymbol{\sigma}_h)\nabla\phi_h \cdot \boldsymbol{\nu}]\!]\right\|_{0,e}^2 \right\}^{1/2} \|\psi\|_{1,\Omega} ,$$

which yields (4.38), concluding the proof. □

Finally, we point out that the reliability of the operator $\boldsymbol{\Theta}$ (cf. upper bound in (4.16)) essentially follows from Theorem 4.10, and Lemmas 4.13 and 4.14.

4.2.2 Efficiency

The goal of this section is to show the efficiency of our a posteriori error estimator $\boldsymbol{\Theta}$. In other words, we now provide upper bounds depending on the actual errors for the nine terms defining the local indicator $\boldsymbol{\Theta}_K$. We begin by establishing the main result of this section.

Theorem 4.15 *There exists $C_{\rm eff} > 0$, independent of λ and h, such that*

$$C_{\rm eff}\boldsymbol{\Theta} \leq \|(\vec{\boldsymbol{\sigma}}, \phi) - (\vec{\boldsymbol{\sigma}}_h, \phi_h)\| \,. \tag{4.39}$$

Throughout this section, as well as Section 4.3.3, we assume for simplicity that the nonlinear functions $\boldsymbol{f}$, g and ϑ are such that $\boldsymbol{f}(\phi_h)$, $g(\boldsymbol{u}_h)$ and $\vartheta(\boldsymbol{\sigma}_h)$, are all piecewise polynomials. The same is assumed for the data $\boldsymbol{u}_{\rm D}$. If this is not the case, but $\boldsymbol{f}$, g, ϑ and $\boldsymbol{u}_{\rm D}$ are sufficiently smooth, higher order terms given by the errors arising from suitable polynomial approximations would appear in the right-hand side of (4.39), (4.63) and (4.67).

In order to prove (4.39), in the rest of this section we derive suitable upper bounds for the terms defining the local error indicator $\boldsymbol{\Theta}_K$ (cf. (4.13) - (4.14)). We begin by observing, thanks to the fact that $-\mathbf{div}\,\boldsymbol{\sigma} = \boldsymbol{f}(\phi)$ in Ω, that there hold

$$\begin{aligned} \|\boldsymbol{f}(\phi_h) + \mathbf{div}\,\boldsymbol{\sigma}_h\|^2_{0,K} &\leq 2\,\|\boldsymbol{f}(\phi) - \boldsymbol{f}(\phi_h)\|^2_{0,K} + 2\,\|\mathbf{div}\,(\boldsymbol{\sigma} - \boldsymbol{\sigma}_h)\|^2_{0,K} \\ &\leq 2L_f^2\,\|\phi - \phi_h\|^2_{0,K} + 2\,\|\mathbf{div}\,(\boldsymbol{\sigma} - \boldsymbol{\sigma}_h)\|^2_{0,K}\,, \end{aligned} \tag{4.40}$$

and

$$\|\boldsymbol{\sigma}_h - \boldsymbol{\sigma}_h^{\rm t}\|^2_{0,K} \leq 4\,\|\boldsymbol{\sigma} - \boldsymbol{\sigma}_h\|^2_{0,K}\,. \tag{4.41}$$

The following lemmas provide the corresponding upper bounds for the remaining estimates required to obtain the efficiency of $\boldsymbol{\Theta}$.

Lemma 4.16 *There exist $C_3, C_4 > 0$, independent of λ and h, such that*

$$h_K^2\,\left\|\mathbf{curl}\,(\mathcal{C}^{-1}\boldsymbol{\sigma}_h + \boldsymbol{\rho}_h)\right\|^2_{0,K} \leq C_3\left\{\|\boldsymbol{\sigma} - \boldsymbol{\sigma}_h\|^2_{0,K} + \|\boldsymbol{\rho} - \boldsymbol{\rho}_h\|^2_{0,K}\right\} \quad \forall\, K \in \mathcal{T}_h, \tag{4.42}$$

and

$$h_e\,\left\|[\![(\mathcal{C}^{-1}\boldsymbol{\sigma}_h + \boldsymbol{\rho}_h + c\mathbb{I})\boldsymbol{s}]\!]\right\|^2_{0,e} \leq C_4\left\{\|\boldsymbol{\sigma} - \boldsymbol{\sigma}_h\|^2_{0,\omega_e} + \|\boldsymbol{\rho} - \boldsymbol{\rho}_h\|^2_{0,\omega_e}\right\} \quad \forall\, e \in \mathcal{E}_h(\Omega).$$

Proof. It suffices to apply Lemma 4.7 with $\boldsymbol{\xi}_h := \mathcal{C}^{-1}\boldsymbol{\sigma}_h + \boldsymbol{\rho}_h + c\mathbb{I}$ and $\boldsymbol{\xi} := \mathcal{C}^{-1}\boldsymbol{\sigma} + \boldsymbol{\rho} + c\mathbb{I}$. □

Lemma 4.17 *There exists $C_5 > 0$, independent of λ and h, such that for each $K \in \mathcal{T}_h$, there holds*

$$h_K^2\,\left\|\nabla\boldsymbol{u}_h - \left(\mathcal{C}^{-1}\boldsymbol{\sigma}_h + \boldsymbol{\rho}_h + c\mathbb{I}\right)\right\|^2_{0,K} \leq C_5\left\{\|\boldsymbol{u} - \boldsymbol{u}_h\|^2_{0,K} + h_K^2\,\|\boldsymbol{\sigma} - \boldsymbol{\sigma}_h\|^2_{0,K} + h_K^2\,\|\boldsymbol{\rho} - \boldsymbol{\rho}_h\|^2_{0,K}\right\}.$$

Proof. It follows from an application of (4.9) with $\boldsymbol{q} := \nabla\boldsymbol{u}_h - (\mathcal{C}^{-1}\boldsymbol{\sigma}_h + \boldsymbol{\rho}_h + c\mathbb{I})$, the estimate (3.3) and then, the use of Lemma 4.5. We refer to [24, Lemma 4.12] and [13, Lemma 6.6] for further details. □

Lemma 4.18 *There exists $C_6 > 0$, independent of λ and h, such that for each $e \in \mathcal{E}_h(\Gamma)$, there holds*

$$h_e\left\|\frac{d\boldsymbol{u}_{\rm D}}{d\boldsymbol{s}} - (\mathcal{C}^{-1}\boldsymbol{\sigma}_h + \boldsymbol{\rho}_h + c\mathbb{I})\boldsymbol{s}\right\|^2_{0,e} \leq C_6\left\{\|\boldsymbol{\sigma} - \boldsymbol{\sigma}_h\|^2_{0,K_e} + \|\boldsymbol{\rho} - \boldsymbol{\rho}_h\|^2_{0,K_e}\right\},$$

where K_e is the triangle of $\mathcal{T}_h$ having e as an edge.

Proof. We begin by defining $\boldsymbol{\xi}$, $\boldsymbol{\xi}_h$ as in the proof of Lemma 4.16, and then, given $e \in \mathcal{E}_h(\Gamma)$, we denote $\boldsymbol{\chi}_e := \frac{d\boldsymbol{u}_{\rm D}}{d\boldsymbol{s}} - \boldsymbol{\xi}_h\boldsymbol{s}$ on e. Thus, applying the inequality (4.10) to $\boldsymbol{\chi}_e$, the extension operator $\mathbf{L} : \mathbf{C}(e) \to \mathbf{C}(K)$ and the fact that $\frac{d\boldsymbol{u}_{\rm D}}{d\boldsymbol{s}} = \nabla\boldsymbol{u}\boldsymbol{s}$, we obtain

$$\|\boldsymbol{\chi}_e\|^2_{0,e} \leq c_4\|\psi_e^{1/2}\boldsymbol{\chi}_e\|^2_{0,e} = c_4\int_e \psi_e\,\boldsymbol{\chi}_e\cdot\left\{\frac{d\boldsymbol{u}_{\rm D}}{ds} - \boldsymbol{\xi}_h\boldsymbol{s}\right\} = c_4\int_{\partial K_e}\psi_e\,\mathbf{L}(\boldsymbol{\chi}_e)\cdot\left\{(\nabla\boldsymbol{u} - \boldsymbol{\xi}_h)\boldsymbol{s}\right\}.$$

Then, we integrate by parts and use that $\boldsymbol{\xi} = \nabla \boldsymbol{u}$ in Ω (cf. (3.3)), to obtain

$$\int_{\partial K_e} \psi_e \, \mathbf{L}(\boldsymbol{\chi}_e) \cdot \Big\{ (\nabla \boldsymbol{u} - \boldsymbol{\xi}_h) \boldsymbol{s} \Big\} = \int_{K_e} (\boldsymbol{\xi} - \boldsymbol{\xi}_h) : \underline{\mathbf{curl}}(\psi_e \, \mathbf{L}(\boldsymbol{\chi}_e)) + \int_{K_e} \mathbf{curl}(\boldsymbol{\xi}_h) \cdot \psi_e \, \mathbf{L}(\boldsymbol{\chi}_e).$$

Finally, by exploiting the Cauchy-Schwarz inequality, Lemmas 4.5 and 4.7, and then, invoking the estimates (4.11) and (4.42), we obtain the desired result. □

Lemma 4.19 *There exists $C_7 > 0$, independent of λ and h, such that for each $e \in \mathcal{E}_h(\Gamma)$, there holds*

$$h_e \, \|\boldsymbol{u}_{\mathrm{D}} - \boldsymbol{u}_h\|^2_{0,e} \leq C_7 \Big\{ \|\boldsymbol{u} - \boldsymbol{u}_h\|^2_{0,K_e} + h^2_{K_e} \, \|\boldsymbol{\sigma} - \boldsymbol{\sigma}_h\|^2_{0,K_e} + h^2_{K_e} \, \|\boldsymbol{\rho} - \boldsymbol{\rho}_h\|^2_{0,K_e} \Big\} .$$

Proof. It follows from an application of the discrete trace inequality (4.12), the estimate (3.3) and the fact that $\boldsymbol{u} = \boldsymbol{u}_{\mathrm{D}}$ on Γ. We refer to [24, Lemma 4.14] for further details. □

Lemma 4.20 *There exists $C_8 > 0$, independent of h, such that for each $K \in \mathcal{T}_h$, there holds*

$$h^2_K \, \|\mathrm{div}\,(\vartheta(\boldsymbol{\sigma}_h) \nabla \phi_h) + g(\boldsymbol{u}_h)\|^2_{0,K} \leq C_8 \Big\{ h^2_K \, \|\boldsymbol{u} - \boldsymbol{u}_h\|^2_{0,K} + \|\boldsymbol{\sigma} - \boldsymbol{\sigma}_h\|^2_{0,K} + \|\phi - \phi_h\|^2_{1,K} \Big\} .$$

Proof. Proceeding as in [10, Lemma 4.4], given $K \in \mathcal{T}_h$, we define

$$\chi_K := \mathrm{div}\,(\vartheta(\boldsymbol{\sigma}_h) \nabla \phi_h) + g(\boldsymbol{u}_h) \ \text{ on } \ K.$$

Thus, applying (4.9) with $q = \chi_K$, using that $\mathrm{div}\,(\vartheta(\boldsymbol{\sigma}) \nabla \phi) = -g(\boldsymbol{u})$ in Ω, and integrating by parts, we find that

$$\|\chi_K\|^2_{0,K} \leq c_3 \|\psi_K^{1/2} \chi_K\|^2_{0,K} = c_3 \int_K (g(\boldsymbol{u}_h) - g(\boldsymbol{u})) \psi_K \chi_K + \int_K (\vartheta(\boldsymbol{\sigma}) \nabla \phi - \vartheta(\boldsymbol{\sigma}_h) \nabla \phi_h) \cdot \nabla(\psi_K \chi_K).$$

Now, applying the Cauchy-Schwarz inequality, the Lipschitz continuity of g (cf. (2.4)) and the estimate (4.26), we deduce that there exists $\widetilde{C}_8 > 0$, depending only on data and other constants, all of them independent of h, such that

$$\|\chi_K\|^2_{0,K} \leq \widetilde{C}_8 \Big\{ \|\boldsymbol{u} - \boldsymbol{u}_h\|_{0,K} \, \|\psi_K \chi_K\|_{0,K} + \Big(\|\boldsymbol{\sigma} - \boldsymbol{\sigma}_h\|_{0,K} + \|\phi - \phi_h\|_{1,K} \Big) \, |\psi_K \chi_K|_{1,K} \Big\} .$$

Next, using the inverse inequality provided by Lemma 4.5 and the fact that $0 \leq \psi_K \leq 1$ in K, we find that

$$\|\chi_K\|^2_{0,K} \leq \widetilde{C}_8 \Big\{ \|\boldsymbol{u} - \boldsymbol{u}_h\|_{0,K} + c_6 \, h_K^{-1} \Big(\|\boldsymbol{\sigma} - \boldsymbol{\sigma}_h\|_{0,K} + \|\phi - \phi_h\|_{1,K} \Big) \Big\} \, \|\chi_K\|_{0,K} \, ,$$

which gives

$$h^2_K \, \|\chi_K\|^2_{0,K} \leq C_8 \Big\{ h^2_K \, \|\boldsymbol{u} - \boldsymbol{u}_h\|^2_{0,K} + \|\boldsymbol{\sigma} - \boldsymbol{\sigma}_h\|^2_{0,K} + \|\phi - \phi_h\|^2_{0,K} \Big\} ,$$

completing the proof. □

Lemma 4.21 *There exists $C_9 > 0$, independent of h, such that for each $e \in \mathcal{E}_h(\Omega)$, there holds*

$$h_e \, \|[\![\vartheta(\boldsymbol{\sigma}_h) \nabla \phi_h \cdot \boldsymbol{\nu}]\!]\|^2_{0,e} \leq C_9 \sum_{K \subseteq \omega_e} \Big\{ h^2_K \, \|\boldsymbol{u} - \boldsymbol{u}_h\|^2_{0,K} + \|\boldsymbol{\sigma} - \boldsymbol{\sigma}_h\|^2_{0,K} + \|\phi - \phi_h\|^2_{1,K} \Big\} , \tag{4.43}$$

where ω_e is the union of the two triangles in $\mathcal{T}_h$ having e as an edge.

Proof. Proceeding analogously as in the proof of [10, Lemma 4.5], given $e \in \mathcal{E}_h(\Omega)$, we define

$$\chi_e := [\![\vartheta(\boldsymbol{\sigma}_h)\nabla\phi_h \cdot \boldsymbol{\nu}]\!] \ \text{ on } \ e.$$

Thus, we apply (4.10) with $p = \chi_e$, and the integration by parts formula on each $K \in \omega_e$, to obtain

$$\|\chi_e\|_{0,e}^2 \leq c_4 \|\psi_e^{1/2}\chi_e\|_{0,e}^2 = c_4 \int_e [\![\vartheta(\boldsymbol{\sigma}_h)\nabla\phi_h \cdot \boldsymbol{\nu}]\!]\psi_e \, \mathrm{L}(\chi_e) = c_4 \sum_{K\subseteq\omega_e} \int_{\partial K} \vartheta(\boldsymbol{\sigma}_h)\nabla\phi_h \cdot \boldsymbol{\nu} \, \psi_e \, \mathrm{L}(\chi_e)$$

$$= c_4 \sum_{K\subseteq\omega_e} \left\{ \int_K \vartheta(\boldsymbol{\sigma}_h)\nabla\phi_h \cdot \nabla(\psi_e \, \mathrm{L}(\chi_e)) + \int_K \mathrm{div}(\vartheta(\boldsymbol{\sigma}_h)\nabla\phi_h)\psi_e \, \mathrm{L}(\chi_e) \right\}.$$

Next, using that $\mathrm{div}\,(\vartheta(\boldsymbol{\sigma})\nabla\phi) = -g(\boldsymbol{u})$ in Ω and then, integrating by parts once more, we get

$$\|\chi_e\|_{0,e}^2 \leq c_4 \sum_{K\subseteq\omega_e} \left\{ \int_K (\vartheta(\boldsymbol{\sigma}_h)\nabla\phi_h - \vartheta(\boldsymbol{\sigma})\nabla\phi) \cdot \nabla(\psi_e \, \mathrm{L}(\chi_e)) \right.$$

$$\left. + \int_K (g(\boldsymbol{u}) - g(\boldsymbol{u}_h))\psi_e \, \mathrm{L}(\chi_e) + \int_K (\mathrm{div}\,(\vartheta(\boldsymbol{\sigma}_h)\nabla\phi_h) + g(\boldsymbol{u}_h))\psi_e \, \mathrm{L}(\chi_e) \right\}.$$

Then, employing the Cauchy-Schwarz inequality, the Lipschitz continuity of g, the inverse inequality provided by Lemma 4.5, the fact that $0 \leq \psi_e \leq 1$ in ω_e, and the estimate (4.11), we see that

$$\|\chi_e\|_{0,e}^2 \leq \widetilde{C}_9 \sum_{K\subseteq\omega_e} \left\{ h_K^{-1} \, \|\vartheta(\boldsymbol{\sigma}_h)\nabla\phi_h - \vartheta(\boldsymbol{\sigma})\nabla\phi\|_{0,K} + \|\boldsymbol{u} - \boldsymbol{u}_h\|_{0,K} \right.$$

$$\left. + \|\mathrm{div}\,(\vartheta(\boldsymbol{\sigma}_h)\nabla\phi_h) + g(\boldsymbol{u}_h)\|_{0,K} \right\} h_e^{1/2} \, \|\chi_e\|_{0,K},$$

from which, noting that $h_e \leq h_K$, applying the estimate (4.26) and performing simple algebraic manipulations, we deduce that there exists $\widehat{C}_9 > 0$, depending only on data and other constants, all of them independent of h, such that

$$h_e \, \|\chi_e\|_{0,e}^2 \leq \widehat{C}_9 \sum_{K\subseteq\omega_e} \left\{ \|\boldsymbol{\sigma} - \boldsymbol{\sigma}_h\|_{0,K}^2 + \|\phi - \phi_h\|_{0,K}^2 + h_K^2 \, \|\boldsymbol{u} - \boldsymbol{u}_h\|_{0,K}^2 \right.$$

$$\left. + h_K^2 \, \|\mathrm{div}\,(\vartheta(\boldsymbol{\sigma}_h)\nabla\phi_h) + g(\boldsymbol{u}_h)\|_{0,K}^2 \right\}. \tag{4.44}$$

Finally, (4.44) and the efficiency estimate given by Lemma 4.20 imply (4.43), completing the proof. □

We end this section by observing that the efficiency of the a posteriori error indicator $\boldsymbol{\Theta}$ follows straightforwardly from the estimates (4.40) and (4.41), and Lemmas 4.16 - 4.21.

4.3 A posteriori error analysis for the fully-mixed scheme

In this section we derive two reliable and efficient residual-based a posteriori error estimators for the Galerkin scheme (3.8). We introduce the global a posteriori error estimators

$$\widetilde{\boldsymbol{\Theta}} := \left\{ \sum_{K\in\mathcal{T}_h} \widetilde{\boldsymbol{\Theta}}_K^2 \right\}^{1/2} \quad \text{and} \quad \widehat{\boldsymbol{\Theta}} := \left\{ \sum_{K\in\mathcal{T}_h} \widehat{\boldsymbol{\Theta}}_K^2 \right\}^{1/2},$$

where we define for each $K \in \mathcal{T}_h$

$$\widetilde{\boldsymbol{\Theta}}_K^2 := \boldsymbol{\Theta}_{E,K}^2 + \|\widetilde{\boldsymbol{\sigma}}_h - \vartheta(\boldsymbol{\sigma}_h)\boldsymbol{t}_h\|_{0,K}^2 + \|g(\boldsymbol{u}_h) + \mathrm{div}\,\widetilde{\boldsymbol{\sigma}}_h\|_{0,K}^2 + \|\nabla\phi_h - \boldsymbol{t}_h\|_{0,K}^2,$$

$$\widehat{\boldsymbol{\Theta}}_K^2 := \widetilde{\boldsymbol{\Theta}}_K^2 + h_K^2 \|\mathrm{rot}(\boldsymbol{t}_h)\|_{0,K}^2 + \sum_{e\in\mathcal{E}_h(K)} h_e \, \|[\![\boldsymbol{t}_h \cdot \boldsymbol{s}]\!]\|_{0,e}^2 \,, \tag{4.45}$$

with $\boldsymbol{\Theta}_{E,K}^2$ defined by (4.13).

The main goal of this section is to establish, under suitable assumptions, the existence of positive constants $C_{\mathrm{rel}}, C_{\mathrm{eff}}$, c_{rel}, c_{eff}, independent of the meshsizes and the continuous and discrete solutions, such that

$$C_{\mathrm{eff}}\widetilde{\boldsymbol{\Theta}} \leq \|(\vec{\boldsymbol{\sigma}}, \underline{\widetilde{\boldsymbol{\sigma}}}) - (\vec{\boldsymbol{\sigma}}_h, \underline{\widetilde{\boldsymbol{\sigma}}}_h)\| \leq C_{\mathrm{rel}}\widetilde{\boldsymbol{\Theta}}, \quad \text{and} \quad c_{\mathrm{eff}}\widehat{\boldsymbol{\Theta}} \leq \|(\vec{\boldsymbol{\sigma}}, \underline{\widetilde{\boldsymbol{\sigma}}}) - (\vec{\boldsymbol{\sigma}}_h, \underline{\widetilde{\boldsymbol{\sigma}}}_h)\| \leq c_{\mathrm{rel}}\widehat{\boldsymbol{\Theta}}. \tag{4.46}$$

4.3.1 A general a posteriori error estimate

We now focus here on the mixed diffusion equation. Applying the uniform ellipticity of the bilinear form $A_{\boldsymbol{\sigma}}$, we conclude a preliminary upper bound for the total error under smallness-of-data assumptions. More precisely, we begin with the following auxiliary result.

Lemma 4.22 *There exists $C_2 > 0$, independent of h, such that*

$$\begin{aligned}\|\underline{\widetilde{\boldsymbol{\sigma}}} - \underline{\widetilde{\boldsymbol{\sigma}}}_h\|_{\mathbf{H}_2} \leq C_2\big\{ &\|\mathcal{R}^D\|_{\mathbf{H}(\mathrm{div};\Omega)'} + \|g(\boldsymbol{u}_h) + \mathrm{div}\,\widetilde{\boldsymbol{\sigma}}_h\|_{0,\Omega} + \|\widetilde{\boldsymbol{\sigma}}_h - \vartheta(\boldsymbol{\sigma}_h)\boldsymbol{t}_h\|_{0,\Omega} \\ &+ \|\nabla\phi_h - \boldsymbol{t}_h\|_{0,\Omega} + L_\vartheta\, c_{\mathbf{S}} \left(\|\boldsymbol{u}_{\mathrm{D}}\|_{1/2,\Gamma} + f_2|\Omega|^{1/2}\right) \|\boldsymbol{\sigma} - \boldsymbol{\sigma}_h\|_{\mathbf{div};\Omega} \\ &+ \vartheta_2 \, \|\boldsymbol{t} - \boldsymbol{t}_h\|_{0,\Omega} + L_g \, \|\boldsymbol{u} - \boldsymbol{u}_h\|_{0,\Omega}\big\},\end{aligned} \tag{4.47}$$

where the functional $\mathcal{R}^D$ is defined by

$$\mathcal{R}^D(\widetilde{\boldsymbol{\tau}}) := -\kappa_2 \int_\Omega (g(\boldsymbol{u}_h) + \mathrm{div}\,\widetilde{\boldsymbol{\sigma}}_h) \cdot \mathrm{div}\,\widetilde{\boldsymbol{\tau}} - \int_\Omega \boldsymbol{t}_h \cdot \widetilde{\boldsymbol{\tau}} - \int_\Omega \phi_h \mathrm{div}\,\widetilde{\boldsymbol{\tau}} - \kappa_1 \int_\Omega (\widetilde{\boldsymbol{\sigma}}_h - \vartheta(\boldsymbol{\sigma}_h)\boldsymbol{t}_h) \cdot \widetilde{\boldsymbol{\tau}}, \tag{4.48}$$

for each $\widetilde{\boldsymbol{\tau}} \in \mathbf{H}(\mathrm{div};\Omega)$. Furthermore, there holds

$$\mathcal{R}^D(\widetilde{\boldsymbol{\tau}}_h) = 0 \quad \forall\, \widetilde{\boldsymbol{\tau}}_h \in \mathbf{H}_h^{\widetilde{\boldsymbol{\sigma}}}. \tag{4.49}$$

Proof. We proceed similar as in the proof of Lemma 4.9, applying the global inf-sup condition to the error between $\underline{\widetilde{\boldsymbol{\sigma}}}$ and $\underline{\widetilde{\boldsymbol{\sigma}}}_h$, to obtain

$$\alpha \, \|\underline{\widetilde{\boldsymbol{\sigma}}} - \underline{\widetilde{\boldsymbol{\sigma}}}_h\|_{\mathbf{H}_2} \leq \sup_{\substack{\underline{\widetilde{\boldsymbol{\tau}}}\in\mathbf{H}_2 \\ \underline{\widetilde{\boldsymbol{\tau}}}\neq\mathbf{0}}} \frac{G_{\boldsymbol{u}}(\underline{\widetilde{\boldsymbol{\tau}}}) - A_{\boldsymbol{\sigma}}(\underline{\widetilde{\boldsymbol{\sigma}}}_h, \underline{\widetilde{\boldsymbol{\tau}}})}{\|\underline{\widetilde{\boldsymbol{\tau}}}\|_{\mathbf{H}_2}},$$

where α is the ellipticity constant of $A_{\boldsymbol{\sigma}}$ given in [26, eq. (3.18)]. Now, adding and subtracting terms appropriately, we can write

$$G_{\boldsymbol{u}}(\underline{\widetilde{\boldsymbol{\tau}}}) - A_{\boldsymbol{\sigma}}(\underline{\widetilde{\boldsymbol{\sigma}}}_h, \underline{\widetilde{\boldsymbol{\tau}}}) = G_{\boldsymbol{u}_h}(\underline{\widetilde{\boldsymbol{\tau}}}) - A_{\boldsymbol{\sigma}_h}(\underline{\widetilde{\boldsymbol{\sigma}}}_h, \underline{\widetilde{\boldsymbol{\tau}}}) + A_{\boldsymbol{\sigma}_h}(\underline{\widetilde{\boldsymbol{\sigma}}}_h, \underline{\widetilde{\boldsymbol{\tau}}}) - A_{\boldsymbol{\sigma}}(\underline{\widetilde{\boldsymbol{\sigma}}}_h, \underline{\widetilde{\boldsymbol{\tau}}}) + G_{\boldsymbol{u}}(\underline{\widetilde{\boldsymbol{\tau}}}) - G_{\boldsymbol{u}_h}(\underline{\widetilde{\boldsymbol{\tau}}}). \tag{4.50}$$

In this way, by using the definitions of $A_{\boldsymbol{\sigma}}$, $A_{\boldsymbol{\sigma}_h}$, $G_{\boldsymbol{u}}$, and $G_{\boldsymbol{u}_h}$, we notice that

$$\begin{aligned}|(A_{\boldsymbol{\sigma}_h} - A_{\boldsymbol{\sigma}})(\underline{\widetilde{\boldsymbol{\sigma}}}_h, \underline{\widetilde{\boldsymbol{\tau}}})| \leq \widetilde{C}_2 \Big\{ &L_\vartheta c_{\mathbf{S}} (\|\boldsymbol{u}_{\mathrm{D}}\|_{1/2,\Gamma} + f_2|\Omega|^{1/2}) \, \|\widetilde{\boldsymbol{\sigma}} - \widetilde{\boldsymbol{\sigma}}_h\|_{0,\Omega} \\ &+ \vartheta_2 \, \|\boldsymbol{t} - \boldsymbol{t}_h\|_{0,\Omega} \Big\} \, \|\underline{\widetilde{\boldsymbol{\tau}}}\|_{\mathbf{H}_2} \,,\end{aligned} \tag{4.51}$$

$$|(G_{\boldsymbol{u}} - G_{\boldsymbol{u}_h})(\underline{\widetilde{\boldsymbol{\tau}}})| \leq \widehat{C}_2 L_g \, \|\boldsymbol{u} - \boldsymbol{u}_h\|_{0,\Omega} \, \|\underline{\widetilde{\boldsymbol{\tau}}}\|_{\mathbf{H}_2}, \tag{4.52}$$

and

$$|G_{\boldsymbol{u}_h}(\widetilde{\underline{\boldsymbol{\tau}}}) - A_{\boldsymbol{\sigma}_h}(\widetilde{\underline{\boldsymbol{\sigma}}}_h, \widetilde{\underline{\boldsymbol{\tau}}})| \leq \overline{C}_2 \Big\{ |\mathcal{R}^D(\widetilde{\boldsymbol{\tau}})| + \|g(\boldsymbol{u}_h) + \operatorname{div} \widetilde{\boldsymbol{\sigma}}_h\|_{0,\Omega} + \|\widetilde{\boldsymbol{\sigma}}_h - \vartheta(\boldsymbol{\sigma}_h)\boldsymbol{t}_h\|_{0,\Omega} + \|\nabla\phi_h - \boldsymbol{t}_h\|_{0,\Omega} \Big\} \|\widetilde{\underline{\boldsymbol{\tau}}}\|_{\mathbf{H}_2}, \tag{4.53}$$

and then, the estimate (4.47) follows by replacing (4.51), (4.52) and (4.53) back into (4.50). Finally, using the fact that $G_{\boldsymbol{u}_h}(\widetilde{\underline{\boldsymbol{\tau}}}_h) - A_{\boldsymbol{\sigma}_h}(\widetilde{\underline{\boldsymbol{\sigma}}}_h, \widetilde{\underline{\boldsymbol{\tau}}}_h) = 0 \quad \forall\, \widetilde{\underline{\boldsymbol{\tau}}}_h \in \mathbf{H}_{2,h}$, and taking in particular $\boldsymbol{s}_h = 0$ and $\psi_h = 0$, we arrive at (4.49), which completes the proof. □

Consequently, we can establish the following preliminary upper bound for the total error.

Theorem 4.23 *Assume that*

$$C_1 L_f + C_2 \left\{ L_\vartheta c_{\mathbf{S}} \left(\|\boldsymbol{u}_{\mathrm{D}}\|_{1/2,\Gamma} + f_2 |\Omega|^{1/2} \right) + \vartheta_2 + L_g \right\} < \frac{1}{2}. \tag{4.54}$$

Then, there exists $C_3 > 0$, independent of λ and h, such that the total error satisfies

$$\|(\vec{\boldsymbol{\sigma}}, \widetilde{\underline{\boldsymbol{\sigma}}}) - (\vec{\boldsymbol{\sigma}}_h, \widetilde{\underline{\boldsymbol{\sigma}}}_h)\| \leq C_3 \Big\{ \|\mathcal{R}^E\|_{\mathbb{H}_0(\mathbf{div};\Omega)'} + \|f(\phi_h) + \mathbf{div}\, \boldsymbol{\sigma}_h\|_{0,\Omega} + \|\boldsymbol{\sigma}_h - \boldsymbol{\sigma}_h^{\mathrm{t}}\|_{0,\Omega} + \|\mathcal{R}^D\|_{\mathbf{H}(\mathrm{div};\Omega)'} + \|g(\boldsymbol{u}_h) + \operatorname{div} \widetilde{\boldsymbol{\sigma}}_h\|_{0,\Omega} + \|\widetilde{\boldsymbol{\sigma}}_h - \vartheta(\boldsymbol{\sigma}_h)\boldsymbol{t}_h\|_{0,\Omega} + \|\nabla\phi_h - \boldsymbol{t}_h\|_{0,\Omega} \Big\}.$$

Proof. It follows as a straightforward application of (4.54) and Lemmas 4.8 and 4.22. □

We end this section by rewriting equivalently the residual $\mathcal{R}^D$. In fact, given $\widetilde{\boldsymbol{\tau}} \in \mathbf{H}(\mathrm{div};\Omega)$, we apply integration by parts to the third term on the right-hand side of (4.48), to obtain

$$\mathcal{R}^D(\widetilde{\boldsymbol{\tau}}) = -\kappa_2 \int_\Omega (g(\boldsymbol{u}_h) + \operatorname{div} \widetilde{\boldsymbol{\sigma}}_h) \cdot \operatorname{div} \widetilde{\boldsymbol{\tau}} + \int_\Omega (\nabla\phi_h - \boldsymbol{t}_h) \cdot \widetilde{\boldsymbol{\tau}} - \kappa_1 \int_\Omega (\widetilde{\boldsymbol{\sigma}}_h - \vartheta(\boldsymbol{\sigma}_h)\boldsymbol{t}_h) \cdot \widetilde{\boldsymbol{\tau}}. \tag{4.55}$$

4.3.2 Reliability of the a posteriori error estimators

The main goal of this section is to establish an upper bound for the residual $\mathcal{R}^D$ in its respective norm. This task is actually performed in two different ways, which leads to the reliability of the a posteriori error estimators $\widetilde{\boldsymbol{\Theta}}$ and $\widehat{\boldsymbol{\Theta}}$. We begin with the upper bound for the first inequality in (4.46).

Lemma 4.24 *There exists a constant $C_{\mathrm{rel}} > 0$, independent of λ and h, such that*

$$\|(\vec{\boldsymbol{\sigma}}, \widetilde{\underline{\boldsymbol{\sigma}}}) - (\vec{\boldsymbol{\sigma}}_h, \widetilde{\underline{\boldsymbol{\sigma}}}_h)\| \leq C_{\mathrm{rel}} \widetilde{\boldsymbol{\Theta}}.$$

Proof. The proof follows straightforwardly from the application of the Cauchy-Schwarz inequality to the residual $\mathcal{R}^D$ (cf. (4.55)), Lemma 4.13, and the definition of $\widetilde{\boldsymbol{\Theta}}$. □

In turn, we now aim at establishing an upper bound for the second inequality in (4.46). For that, we will apply the vector form of the Helmholtz decomposition in Lemma 4.8, to bound $\|\mathcal{R}^D\|_{\mathbf{H}(\mathrm{div};\Omega)'}$. In fact, given $\widetilde{\boldsymbol{\tau}} \in \mathbf{H}(\mathrm{div};\Omega)$, there exist $z \in \mathrm{H}^2(\Omega)$ and $\Phi \in \mathrm{H}^1(\Omega)$ such that

$$\widetilde{\boldsymbol{\tau}} = \nabla z + \mathbf{rot}\, \Phi \quad \in \quad \Omega, \quad \text{and} \quad \|z\|_{2,\Omega} + \|\Phi\|_{1,\Omega} \leq C \|\widetilde{\boldsymbol{\tau}}\|_{\mathrm{div};\Omega}, \tag{4.56}$$

and then, denoting $\Phi_h := \mathrm{I}_h(\Phi)$, we define $\widetilde{\boldsymbol{\tau}}_h := \Pi_h(\nabla z) + \mathbf{rot}(\Phi_h) \in \mathbf{H}_h^{\widetilde{\boldsymbol{\sigma}}}$. In this way, noticing from (4.49) that $\mathcal{R}^D(\widetilde{\boldsymbol{\tau}}_h) = 0$, it readily follows that $\mathcal{R}^D(\widetilde{\boldsymbol{\tau}})$ can be decomposed as

$$\mathcal{R}^D(\widetilde{\boldsymbol{\tau}}) = \mathcal{R}^D(\widetilde{\boldsymbol{\tau}} - \widetilde{\boldsymbol{\tau}}_h) = \mathcal{R}^D\big(\nabla z - \Pi_h(\nabla z)\big) + \mathcal{R}^D\big(\mathbf{rot}(\Phi - \Phi_h)\big). \tag{4.57}$$

In the following two lemmas, we provide upper bounds for the terms on the right-hand side of (4.57).

Lemma 4.25 *There exists $C > 0$, independent of h, such that for each $z \in \mathrm{H}^2(\Omega)$, there holds*

$$|\mathcal{R}^D\big(\nabla z - \Pi_h(\nabla z)\big)| \leq C\Big\{ \sum_{K\in\mathcal{T}_h} \Big(\|g(\boldsymbol{u}_h) + \mathrm{div}\,\widetilde{\boldsymbol{\sigma}}_h\|^2_{0,K} + h_K^2\|\nabla\phi_h - \boldsymbol{t}_h\|^2_{0,K} + h_K^2\|\widetilde{\boldsymbol{\sigma}}_h - \vartheta(\boldsymbol{\sigma}_h)\boldsymbol{t}_h\|^2_{0,K}\Big)\Big\}^{1/2} \|z\|_{2,\Omega}\,. \tag{4.58}$$

Proof. Given $z \in \mathrm{H}^2(\Omega)$, we first notice, from the definition of $\mathcal{R}^D$ (cf. (4.55)), that there holds

$$\begin{aligned}\mathcal{R}^D\big(\nabla z - \Pi_h(\nabla z)\big) &= -\kappa_2 \int_\Omega (g(\boldsymbol{u}_h) + \mathrm{div}\,\widetilde{\boldsymbol{\sigma}}_h)\cdot \mathrm{div}\,(\nabla z - \Pi_h(\nabla z)) \\ &\quad + \int_\Omega (\nabla\phi_h - \boldsymbol{t}_h)\cdot(\nabla z - \Pi_h(\nabla z)) - \kappa_1 \int_\Omega (\widetilde{\boldsymbol{\sigma}}_h - \vartheta(\boldsymbol{\sigma}_h)\boldsymbol{t}_h)\cdot(\nabla z - \Pi_h(\nabla z)).\end{aligned} \tag{4.59}$$

For the first term on the right-hand side of (4.59) we proceed as in [5, Lemma 3.10], whereas for the remaining terms, we simply apply the Cauchy-Schwarz inequality, and subsequently use the approximation properties of Π_h provided by Lemma 4.2. □

Lemma 4.26 *There exists $C > 0$, independent of h, such that for each $\Phi \in \mathrm{H}^1(\Omega)$, there holds*

$$|\mathcal{R}^D\big(\mathbf{rot}(\Phi - \Phi_h)\big)| \leq C\left\{ \sum_{K\in\mathcal{T}_h} \left(\|\widetilde{\boldsymbol{\sigma}}_h - \vartheta(\boldsymbol{\sigma}_h)\boldsymbol{t}_h\|^2_{0,K} + h_K^2\|\mathrm{rot}(\boldsymbol{t}_h)\|^2_{0,K} + \sum_{e\in\mathcal{E}_h(K)} h_e\,\|[\![\boldsymbol{t}_h\cdot\boldsymbol{s}]\!]\|^2_{0,e}\right)\right\}^{1/2} \|\Phi\|_{1,\Omega}\,.$$

Proof. Given $\Phi \in \mathrm{H}^1(\Omega)$, we notice from the original definition of $\mathcal{R}^D$ (cf. (4.48)) that there holds

$$\mathcal{R}^D\big(\mathbf{rot}(\Phi - \Phi_h)\big) = -\kappa_1 \int_\Omega (\widetilde{\boldsymbol{\sigma}}_h - \vartheta(\boldsymbol{\sigma}_h)\boldsymbol{t}_h)\cdot\mathbf{rot}(\Phi - \Phi_h) - \int_\Omega \boldsymbol{t}_h\cdot\mathbf{rot}(\Phi - \Phi_h). \tag{4.60}$$

For the first term, we proceed as in the proof of [27, Lemma 3.9], applying the boundedness of $\mathrm{I}_h : \mathrm{H}^1(\Omega) \to \mathrm{H}^1(\Omega)$ (cf. [22, Lemma 1.127]), and the Cauchy-Schwarz and triangle inequalities, to deduce that

$$\left|\kappa_1 \int_\Omega (\widetilde{\boldsymbol{\sigma}}_h - \vartheta(\boldsymbol{\sigma}_h)\boldsymbol{t}_h)\cdot\mathbf{rot}(\Phi - \Phi_h)\right| \leq C_1\|\widetilde{\boldsymbol{\sigma}}_h - \vartheta(\boldsymbol{\sigma}_h)\boldsymbol{t}_h\|_{0,\Omega}\,\|\Phi\|_{1,\Omega}\,. \tag{4.61}$$

Now, for the second term, we proceed as in the proof of [15, Lemma 3.9], to obtain

$$\left|\int_\Omega \boldsymbol{t}_h\cdot\mathbf{rot}(\Phi - \Phi_h)\right| \leq C_2\left\{ \sum_{K\in\mathcal{T}_h} \left(h_K^2\|\mathrm{rot}(\boldsymbol{t}_h)\|^2_{0,K} + \sum_{e\in\mathcal{E}_h(K)} h_e\,\|[\![\boldsymbol{t}_h\cdot\boldsymbol{s}]\!]\|^2_{0,e}\right)\right\}^{1/2} \|\Phi\|_{1,\Omega}\,. \tag{4.62}$$

Finally, the desired result follows by replacing (4.61) and (4.62) back into (4.60). □

As a consequence of Lemmas 4.25 and 4.26, the identity (4.57), and the stability result given by (4.56), we can deduce the required upper bound for $\|\mathcal{R}^D\|_{\mathbf{H}(\mathrm{div};\Omega)'}$, that is

$$\|\mathcal{R}^D\|_{\mathbf{H}(\mathrm{div};\Omega)'} \leq C\left\{ \sum_{K\in\mathcal{T}_h} \Big(\|g(\boldsymbol{u}_h) + \mathrm{div}\,\widetilde{\boldsymbol{\sigma}}_h\|^2_{0,K} + h_K^2\|\nabla\phi_h - \boldsymbol{t}_h\|^2_{0,K} + h_K^2\|\widetilde{\boldsymbol{\sigma}}_h - \vartheta(\boldsymbol{\sigma}_h)\boldsymbol{t}_h\|^2_{0,K}\right.\right.$$

$$+ \|\widetilde{\boldsymbol{\sigma}}_h - \vartheta(\boldsymbol{\sigma}_h)\boldsymbol{t}_h\|^2_{0,K} + h_K^2\|\mathrm{rot}(\boldsymbol{t}_h)\|^2_{0,K} + \sum_{e\in\mathcal{E}_h(K)} h_e\,\|[\![\boldsymbol{t}_h\cdot\boldsymbol{s}]\!]\|^2_{0,e}\Big)\Big\}^{1/2},$$

where C is a positive constant independent of h.

Finally, we point out that the existence of a constant $c_{\mathrm{rel}} > 0$, such that

$$\|(\vec{\boldsymbol{\sigma}},\underline{\widetilde{\boldsymbol{\sigma}}}) - (\vec{\boldsymbol{\sigma}}_h,\underline{\widetilde{\boldsymbol{\sigma}}}_h)\| \le c_{\mathrm{rel}}\widehat{\boldsymbol{\Theta}},$$

follows from Theorem 4.23, and Lemmas 4.13, 4.25 and 4.26, after observing that, for sufficiently small elements, the terms $h_K^2\|\nabla\phi_h - \boldsymbol{t}_h\|^2_{0,K}$ and $h_K^2\|\widetilde{\boldsymbol{\sigma}}_h - \vartheta(\boldsymbol{\sigma}_h)\boldsymbol{t}_h\|^2_{0,K}$ in (4.58), are dominated by $\|\nabla\phi_h - \boldsymbol{t}_h\|^2_{0,K}$ and $\|\widetilde{\boldsymbol{\sigma}}_h - \vartheta(\boldsymbol{\sigma}_h)\boldsymbol{t}_h\|^2_{0,K}$, respectively.

4.3.3 Efficiency of the a posteriori error estimators

Let us begin with the efficiency estimate for $\widetilde{\boldsymbol{\Theta}}$.

Lemma 4.27 *There exists $C_{\mathrm{eff}} > 0$, independent of λ and h, such that*

$$C_{\mathrm{eff}}\widetilde{\boldsymbol{\Theta}} \le \|(\vec{\boldsymbol{\sigma}},\underline{\widetilde{\boldsymbol{\sigma}}}) - (\vec{\boldsymbol{\sigma}}_h,\underline{\widetilde{\boldsymbol{\sigma}}}_h)\|. \tag{4.63}$$

Proof. We recall that $g(\boldsymbol{u}) = -\mathrm{div}\,\widetilde{\boldsymbol{\sigma}}$ in Ω. In this way, it is clear that

$$\|g(\boldsymbol{u}_h) + \mathrm{div}\,\widetilde{\boldsymbol{\sigma}}_h\|^2_{0,K} \le 2\,\|\mathrm{div}(\widetilde{\boldsymbol{\sigma}} - \widetilde{\boldsymbol{\sigma}}_h)\|^2_{0,K} + 2L_g^2\,\|\boldsymbol{u} - \boldsymbol{u}_h\|^2_{0,K}\,. \tag{4.64}$$

Moreover, since $\widetilde{\boldsymbol{\sigma}} = \vartheta(\boldsymbol{\sigma})\boldsymbol{t}$ in Ω, applying the Lipschitz continuity of ϑ, the regularity estimate [25, eq. (2.23)], and the Cauchy-Schwarz inequality, we deduce

$$\|\widetilde{\boldsymbol{\sigma}}_h - \vartheta(\boldsymbol{\sigma}_h)\boldsymbol{t}_h\|^2_{0,K} \le C\Big\{\|\widetilde{\boldsymbol{\sigma}} - \widetilde{\boldsymbol{\sigma}}_h\|^2_{0,K} + \|\boldsymbol{\sigma} - \boldsymbol{\sigma}_h\|^2_{0,K} + \|\boldsymbol{t} - \boldsymbol{t}_h\|^2_{0,K}\Big\}. \tag{4.65}$$

Additionally, since $\boldsymbol{t} = \nabla\phi$ in Ω, we get

$$\|\nabla\phi_h - \boldsymbol{t}_h\|^2_{0,K} \le C_1\Big\{\|\phi - \phi_h\|^2_{1,K} + \|\boldsymbol{t} - \boldsymbol{t}_h\|^2_{0,K}\Big\}. \tag{4.66}$$

Finally, the result follows from the definition of $\widetilde{\boldsymbol{\Theta}}$, estimates (4.40), (4.41), (4.64), (4.65) and (4.66), and Lemmas 4.16 - 4.19. □

On the other hand, we derive the efficiency of the estimator $\widehat{\boldsymbol{\Theta}}$. The following lemma provides the required upper bounds for the second and third terms on the right-hand side of (4.45).

Lemma 4.28 *There exist $c_1, c_2 > 0$, independent of h, such that*

$$h_K^2\,\|\mathrm{rot}(\boldsymbol{t}_h)\|^2_{0,K} \le c_1\,\|\boldsymbol{t} - \boldsymbol{t}_h\|^2_{0,K} \quad \forall\, K\in\mathcal{T}_h,$$

$$h_e\,\|[\![\boldsymbol{t}_h\cdot\boldsymbol{s}]\!]\|^2_{0,e} \le c_2\,\|\boldsymbol{t} - \boldsymbol{t}_h\|^2_{0,\omega_e} \quad \forall\, e\in\mathcal{E}_h.$$

Proof. For the first inequality, we simply apply the vector version of the first inequality in Lemma 4.7 with $\boldsymbol{\xi}_h = \boldsymbol{t}_h$ and $\boldsymbol{\xi} = \boldsymbol{t} = \nabla\phi$, whereas for the second one, we can follow the proof given by [11, Lemma 4.4]. We omit further details. □

Finally, as a consequence of the estimates (4.40), (4.41), (4.64), (4.65) and (4.66), and Lemmas 4.16 - 4.19, and 4.28, we are now in position to state the efficiency of $\widehat{\boldsymbol{\Theta}}$.

Lemma 4.29 *There exists a $c_{\mathrm{eff}} > 0$, independent of λ and h, such that*

$$c_{\mathrm{eff}}\widehat{\boldsymbol{\Theta}} \le \|(\vec{\boldsymbol{\sigma}},\underline{\widetilde{\boldsymbol{\sigma}}}) - (\vec{\boldsymbol{\sigma}}_h,\underline{\widetilde{\boldsymbol{\sigma}}}_h)\|. \tag{4.67}$$

5 Numerical results

In this section we present some numerical results illustrating the properties of the estimator introduced in Section 4 and showing the behaviour of the associated adaptive algorithm. The individual errors and rates of convergence of the unknowns will be computed as usual

$$\mathrm{e}(\boldsymbol{\sigma}) = \|\boldsymbol{\sigma} - \boldsymbol{\sigma}_h\|_{\mathbf{div};\Omega}\,,\ \mathrm{e}(\boldsymbol{u}) = \|\boldsymbol{u} - \boldsymbol{u}_h\|_{0,\Omega}\,,\ \mathrm{e}(\boldsymbol{\rho}) = \|\boldsymbol{\rho} - \boldsymbol{\rho}_h\|_{0,\Omega}\,,\ \mathrm{e}(\widetilde{\boldsymbol{\sigma}}) = \|\widetilde{\boldsymbol{\sigma}} - \widetilde{\boldsymbol{\sigma}}_h\|_{\mathrm{div};\Omega}\,,$$

$$\mathrm{e}(\boldsymbol{t}) = \|\boldsymbol{t} - \boldsymbol{t}_h\|_{0,\Omega}\,,\ \mathrm{e}(\phi) = \|\phi - \phi_h\|_{1,\Omega}\,,\ r(\cdot) = \frac{\log(\mathrm{e}(\cdot)/\widehat{\mathrm{e}}(\cdot))}{\log(h/\widehat{h})},$$

where e and $\widehat{\mathrm{e}}$ denote errors computed on two consecutive meshes of sizes h and $\widehat{h}$. When the adaptive algorithm is applied, the expression $\log(h/\widehat{h})$ appearing in the computation of the above rates is replaced by $-0.5\log(N/\widehat{N})$, where N and $\widehat{N}$, denote the corresponding degrees of freedom of each triangulation. In addition, given the total errors

$$\mathrm{e}_1 = \left\{[\mathrm{e}(\boldsymbol{\sigma})]^2 + [\mathrm{e}(\boldsymbol{u})]^2 + [\mathrm{e}(\boldsymbol{\rho})]^2 + [\mathrm{e}(\phi)]^2\right\}, \quad \text{and} \quad \mathrm{e}_2 = \{e_1 + \mathrm{e}[(\boldsymbol{t})]^2 + \mathrm{e}[(\widetilde{\boldsymbol{\sigma}})]^2\},$$

the effectivity indexes associated with $\boldsymbol{\Theta}$, $\widetilde{\boldsymbol{\Theta}}$, and $\widehat{\boldsymbol{\Theta}}$ are defined, respectively, as

$$\mathrm{eff}(\boldsymbol{\Theta}) = \frac{\mathrm{e}_1}{\boldsymbol{\Theta}}, \quad \mathrm{eff}(\widetilde{\boldsymbol{\Theta}}) = \frac{\mathrm{e}_2}{\widetilde{\boldsymbol{\Theta}}}, \quad \text{and} \quad \mathrm{eff}(\widehat{\boldsymbol{\Theta}}) = \frac{\mathrm{e}_2}{\widehat{\boldsymbol{\Theta}}}.$$

The linearisation of the systems associated with the assembled forms of (3.4) and (3.8) is carried out by Newton's method. In turn, the solution of the resulting linear systems at each Newton step are conducted using the Multifrontal Massively Parallel Sparse direct Solver (MUMPS). In addition, the examples use a classical adaptive mesh refinement procedure based on the equi-distribution of the error indicators, where the diameter of each element in the new adapted mesh (contained in a generic element K on the initial coarse mesh) is proportional to the diameter of the initial element times the ratio $\widehat{\boldsymbol{\Theta}}_h/\boldsymbol{\Theta}_K$, where $\widehat{\boldsymbol{\Theta}}_h$ is the mean value of a given indicator $\boldsymbol{\Theta}$ over the initial mesh (cf. [37]).

On the other hand, we recall that given the Young modulus E and the Poisson ratio ν of an isotropic linear elastic solid, the corresponding Lamé parameters are defined as $\lambda = E\nu(1+\nu)^{-1}(1-2\nu)^{-1}$ and $\mu = E/(2+2\nu)$. Thus, in the following examples, we will consider $E = 1.0e3$ and $\nu = 0.4$.

Moreover, we point out that given $D_0 = D_1 = 0.1$, the nonlinear functions

$$\vartheta(\boldsymbol{\sigma}) = (D_0 + D_1(1+|\boldsymbol{\sigma}|^2)^{-0.5})\,\mathbb{I}, \quad \boldsymbol{f}(\phi) = \begin{pmatrix} -\sin(\phi) \\ \cos(\phi) \end{pmatrix}, \quad \text{and} \quad g(\boldsymbol{u}) = 2 + \frac{1}{1+|\boldsymbol{u}|^2},$$

satisfying (2.2)-(2.4), will be used in the following computational tests, and remark that for the examples described below, the elasticity and diffusion equations are considered non-homogeneous and the extra source terms are chosen according to the given exact solutions. This treatment does not compromise the analysis, as the regularity of the exact solution provides sufficiently smooth right-hand sides, thus only requiring a slight modification of the functionals in the variational formulation.

Finally, for the nonlinear diffusivity, the parameters appearing in (2.2) are given by: $\vartheta_0 = D_0$, $\vartheta_2 = \sqrt{2}(D_0 + D_1)$, and then, according to [26, eq. (3.20)], the stabilisation parameters for the fully-mixed scheme (3.8) can be taken as $\kappa_1 = \vartheta_0/\vartheta_2$, $\kappa_2 = \vartheta_0/2\vartheta_2$ and $\kappa_3 = \vartheta_0/2$.

Example 1. In the first example, we consider the following exact solutions to (2.1):

$$\boldsymbol{u} = \frac{1}{\lambda}\begin{pmatrix} d_1\cos(\pi x_1)\sin(2\pi x_2) \\ -d_1\sin(\pi x_1)\cos(\pi x_2) \end{pmatrix}, \quad \phi = 1.0 - e^{-x_1(x_1-1)x_2(x_2-1)}, \tag{5.1}$$

N	e($\boldsymbol{\sigma}$)	$r(\boldsymbol{\sigma})$	e($\boldsymbol{u}$)	$r(\boldsymbol{u})$	e($\boldsymbol{\rho}$)	$r(\boldsymbol{\rho})$	e(ϕ)	$r(\phi)$	eff($\boldsymbol{\Theta}$)
Lowest-order mixed-primal method									
346	0.372	-	8.4e-6	-	3.3e-5	-	5.8e-2	-	1.00
1298	0.191	1.00	4.2e-6	1.03	1.6e-5	1.05	2.8e-2	1.10	0.99
5026	0.096	1.01	2.1e-6	1.01	8.4e-6	1.02	1.4e-2	1.01	0.99
19778	0.048	1.00	1.0e-6	1.01	4.2e-6	1.01	7.0e-3	1.01	0.99
78466	0.024	1.00	5.3e-7	1.00	2.1e-6	1.00	3.5e-3	1.00	0.99
312578	0.012	1.00	2.6e-7	1.00	1.0e-6	1.00	1.7e-3	1.00	0.99
Second-order mixed-primal method									
898	0.0825	-	1.7e-6	-	7.6e-6	-	8.2e-3	-	0.99
3458	0.0213	2.00	4.4e-7	2.01	1.9e-6	2.03	2.1e-3	2.02	0.98
13570	0.0053	2.01	1.1e-7	2.01	4.8e-7	2.02	5.2e-4	2.00	0.98
53762	0.0013	2.01	2.8e-8	2.01	1.2e-7	2.01	1.3e-4	2.01	0.98
214018	0.0003	2.00	7.0e-9	2.00	3.0e-8	2.00	3.2e-5	2.00	0.98

Table 5.1: Example 1: Degrees of freedom, individual absolute errors, rates of convergence, and effectivity index for the first- and second-order mixed-primal finite element methods.

Lowest-order augmented fully-mixed scheme														
N	e($\boldsymbol{\sigma}$)	$r(\boldsymbol{\sigma})$	e($\boldsymbol{u}$)	$r(\boldsymbol{u})$	e($\boldsymbol{\rho}$)	$r(\boldsymbol{\rho})$	e($\widetilde{\boldsymbol{\sigma}}$)	$r(\widetilde{\boldsymbol{\sigma}})$	e($\boldsymbol{t}$)	$r(\boldsymbol{t})$	e(ϕ)	$r(\phi)$	eff($\widetilde{\boldsymbol{\Theta}}$)	eff($\widehat{\boldsymbol{\Theta}}$)
466	3.728	-	8.4e-5	-	3.3e-4	-	1.9e-2	-	4.5e-2	-	5.6e-2	-	1.001	1.00
1762	1.918	0.99	4.2e-5	1.02	1.6e-4	1.05	9.6e-3	1.02	2.3e-2	0.99	2.7e-2	1.08	0.999	0.999
6850	0.965	1.01	2.1e-5	1.01	8.4e-5	1.02	4.7e-3	1.03	1.1e-2	1.00	1.4e-2	0.99	0.999	0.998
27010	0.483	1.00	1.0e-5	1.00	4.2e-5	1.01	2.3e-3	1.01	5.8e-3	1.00	7.0e-3	0.99	0.999	0.998
107266	0.242	1.00	5.3e-6	1.00	2.1e-5	1.00	1.1e-3	1.00	2.9e-3	1.00	3.5e-3	1.00	0.999	0.998
427522	0.121	1.00	2.6e-6	1.00	1.0e-5	1.00	5.9e-4	1.00	1.4e-3	1.00	1.7e-3	1.00	0.999	0.998
Second-order augmented fully-mixed scheme														
1266	0.825	-	1.7e-5	-	7.6e-5	-	2.4e-3	-	6.6e-3	-	7.4e-3	-	1.000	0.997
4898	0.213	1.99	4.4e-6	2.00	1.9e-5	2.02	6.2e-4	2.04	1.7e-3	1.99	1.9e-3	1.96	0.999	0.996
19266	0.053	2.01	1.1e-6	2.01	4.8e-6	2.02	1.5e-4	2.02	4.3e-4	2.01	5.0e-4	1.98	0.999	0.996
76418	0.013	2.00	2.8e-7	2.00	1.2e-6	2.01	3.9e-5	2.01	1.0e-4	2.00	1.2e-4	1.98	0.999	0.996
304386	0.003	2.00	7.0e-8	2.00	3.0e-7	2.00	9.8e-6	2.00	2.7e-5	2.00	3.2e-5	1.99	0.999	0.996

Table 5.2: Example 1: Degrees of freedom, individual absolute errors, rates of convergence, and effectivity indexes for the first- and second-order augmented fully-mixed finite element methods.

defined on the unit square $\Omega = (0,1)^2$, satisfying the boundary conditions $\boldsymbol{u}_{\mathrm{D}} = \boldsymbol{u}$ on Γ and $\phi = 0$ on Γ. The involved coefficient in (5.1) is taken as $d_1 = 0.05$.

The manufactured solutions on the considered domain are smooth, and the a posteriori error indicators show effectivity indexes close to one. The results reported in Tables 5.1 and 5.2 indicate optimal convergence rates for the two lowest-order methods. Approximate solutions obtained after seven steps of uniform refinement are depicted in Figure 5.1.

Example 2. In our second example we design a mesh convergence test using a closed-form solution, and performing uniform and adaptive mesh refinements. Thus, we consider the same computational domain as the one given in Example 1, and propose the following exact solutions

$$\boldsymbol{u} = \frac{1}{\lambda}\begin{pmatrix} \frac{-d_1\sin(x_1)\cos(x_2)}{(x_2+0.02)^2+(x_1+0.02)^2} \\ -d_1\cos(x_1)\sin(2x_2) \end{pmatrix}, \quad \phi = \frac{x_1(x_1-1)x_2(x_2-1)}{(10x_1+0.1)^2}, \tag{5.2}$$

where the manufactured displacement is used as Dirichlet datum on Γ, and the involved coefficient

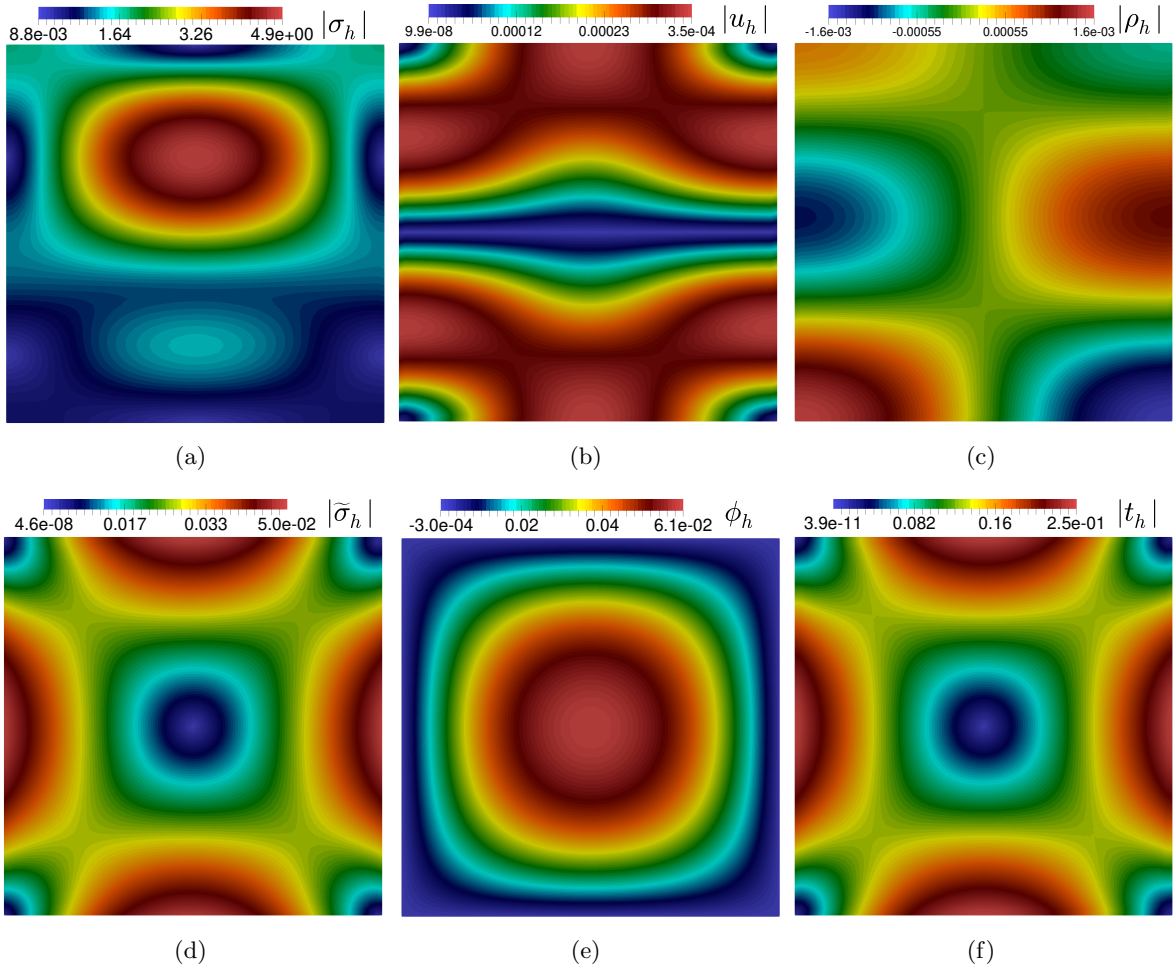

Fig. 5.1: Example 1: Approximation of the stress magnitude $|\boldsymbol{\sigma}_h|$ (a), displacement magnitude $|\boldsymbol{u}_h|$ (b), rotation magnitude $|\boldsymbol{\rho}_h|$ (c), diffusive flux magnitude $|\widetilde{\boldsymbol{\sigma}}_h|$ (d), concentration of the diffusive substance ϕ_h (e), and concentration gradient magnitude $|\boldsymbol{t}_h|$ (f), by using the lowest-order augmented fully-mixed scheme with adaptive refinement according to $\widetilde{\boldsymbol{\Theta}}$.

in (5.2) is taken as in Example 1. Notice that the first component of the displacement, and the concentration, in (5.2), exhibit singularities just outside the domain, at $(0,0)$ and the line $x_1 = -0.01$, respectively, therefore, high gradients are also expected in the approximation of these fields, and optimal convergence is no longer evidenced under uniform mesh refinement (see second row of Tables 5.3 and 5.4). In Tables 5.3 and 5.4, we show the individual errors, the effectivity indexes and experimental rates of convergence for the uniform and adaptive refinements of the mixed-primal and augmented fully-mixed schemes. As expected, we observe that the errors decrease faster through the adaptive procedure, and that in each case, the effectivity indexes remain bounded, which confirms the reliability and efficiency of $\boldsymbol{\Theta}$, $\widetilde{\boldsymbol{\Theta}}$ and $\widehat{\boldsymbol{\Theta}}$, in the cases of non-smooth solutions. Moreover, although super-convergence of the concentration can be seen when the adaptive scheme is applied for the augmented fully-mixed system (see the last two blocks of Table 5.4), we notice from Figure 5.3(a) that the global rate of convergence remains optimal. Furthermore, it is important to remark that when the adaptive algorithms are applied, optimal convergence can be restored, as shown in the last block of Table 5.3 and the last two blocks of Table 5.4. Additionally, we display in Figure 5.2 some

N	e($\boldsymbol{\sigma}$)	$r(\boldsymbol{\sigma})$	e($\boldsymbol{u}$)	$r(\boldsymbol{u})$	e($\boldsymbol{\rho}$)	$r(\boldsymbol{\rho})$	e(ϕ)	$r(\phi)$	eff($\boldsymbol{\Theta}$)
Lowest-order mixed-primal scheme upon uniform refinement									
346	136.2	-	3.4e-5	-	2.2e-4	-	1.54	-	1.13
1298	77.45	0.85	2.4e-5	0.50	2.6e-4	-0.23	1.10	0.50	1.06
5026	56.68	0.46	1.1e-5	1.19	1.8e-4	0.48	0.81	0.45	1.00
19778	42.11	0.43	4.3e-6	1.37	9.9e-5	0.93	0.66	0.30	0.99
78466	26.29	0.68	1.8e-6	1.21	4.3e-5	1.19	0.56	0.24	0.99
312578	14.25	0.88	8.8e-7	1.08	1.8e-5	1.24	0.41	0.42	0.99
Lowest-order mixed-primal scheme with adaptive refinement according to $\boldsymbol{\Theta}$									
346	136.2	-	3.4e-5	-	2.2e-4	-	1.54	-	1.13
898	77.45	1.18	2.3e-5	0.81	2.1e-4	0.46	1.10	0.71	1.06
2239	56.68	0.68	1.0e-5	1.76	1.5e-4	0.70	0.80	0.67	1.00
4985	42.06	0.74	4.5e-6	2.08	8.5e-5	1.56	0.65	0.52	0.99
10968	25.83	1.23	2.8e-6	1.15	4.0e-5	1.88	0.54	0.44	0.99
27366	13.32	1.44	1.7e-6	1.07	1.9e-5	1.62	0.40	0.66	0.99
77382	6.484	1.38	1.1e-6	0.75	9.4e-6	1.36	0.24	0.94	0.99
244093	3.190	1.23	6.5e-7	1.05	4.7e-6	1.21	0.13	1.08	0.99

Table 5.3: Example 2: Degrees of freedom, individual absolute errors, rates of convergence, and effectivity index for the lowest-order mixed-primal finite element method.

adapted meshes obtained during the adaptive refinements according to $\boldsymbol{\Theta}$, $\widetilde{\boldsymbol{\Theta}}$ and $\widehat{\boldsymbol{\Theta}}$, and observe that they are concentrated around $(0,0)$ and the line $x_1 = -0.01$, which shows how the method is able to identify the regions in which the accuracy of the numerical approximation is deteriorated. Finally, approximation solutions are shown in Figure 5.3(b-e) after eight steps of adaptive refinement according to the indicator $\boldsymbol{\Theta}$.

References

[1] S. Agmon, *Lectures on Elliptic Boundary Value Problems*. Van Nostrand, Princeton, New Jersey, 1965.

[2] E.C. Aifantis, *On the problem of diffusion in solids*. Acta Mech. 37 (1980), no. 3-4, 265–296.

[3] M. Ainsworth and J.T. Oden, *A posteriori error estimation in finite element analysis*. Comput. Methods Appl. Mech. Engrg. 142 (1997), no. 1-2, 1–88.

[4] A. Alonso, *Error estimators for a mixed method*. Numer. Math. 74 (1996), no. 4, 385–395.

[5] M. Alvarez, G.N. Gatica, and R. Ruiz-Baier, *A posteriori error analysis for a viscous flow-transport problem*. ESAIM: Math. Model. Numer. Anal. 50 (2016), no. 6, 1789–1816.

[6] M. Alvarez, G.N. Gatica, and R. Ruiz-Baier, *A posteriori error analysis of a fully-mixed formulation for the Brinkman-Darcy problem*. Calcolo 54 (2017), no. 4, 1491–1519.

[7] M. Alvarez, G.N. Gatica, and R. Ruiz-Baier, *A posteriori error estimation for an augmented mixed-primal method applied to sedimentation-consolidation systems*. J. Comput. Phys. 367 (2018), 322–346.

[8] D.N. Arnold, F. Brezzi, and J. Douglas, *PEERS: A new mixed finite element method for plane elasticity*. Jpn J. Appl. Math. 1 (1984), no. 2, 347–367.

[9] D.N. Arnold, R.S. Falk, and R. Winther, *Mixed finite element methods for linear elasticity with weakly imposed symmetry*. Math. Comp. 76 (2007), no. 260, 1699–1723.

N	e($\boldsymbol{\sigma}$)	$r(\boldsymbol{\sigma})$	e($\boldsymbol{u}$)	$r(\boldsymbol{u})$	e($\boldsymbol{\rho}$)	$r(\boldsymbol{\rho})$	e($\widetilde{\boldsymbol{\sigma}}$)	$r(\widetilde{\boldsymbol{\sigma}})$	e($\boldsymbol{t}$)	$r(\boldsymbol{t})$	e(ϕ)	$r(\phi)$	eff($\widetilde{\boldsymbol{\Theta}}$)	eff($\widehat{\boldsymbol{\Theta}}$)
Lowest order augmented fully-mixed scheme upon uniform refinement														
466	136.2	-	3.2e-5	-	2.2e-4	-	130.1	-	17.2	-	48.1	-	1.14	1.11
1762	77.46	0.84	2.1e-5	0.64	2.5e-4	-0.22	91.73	0.52	6.85	1.39	17.1	1.55	1.09	1.08
6850	56.68	0.46	1.0e-5	1.08	1.8e-4	0.46	65.41	0.49	2.84	1.29	6.64	1.39	1.05	1.04
27010	42.11	0.43	4.1e-6	1.28	9.8e-5	0.92	48.19	0.44	1.53	0.89	3.16	1.08	1.02	1.02
107266	26.29	0.68	1.8e-6	1.16	4.3e-5	1.18	37.02	0.38	0.95	0.69	1.66	0.93	1.00	1.00
427522	14.25	0.88	8.9e-7	1.07	1.8e-5	1.24	26.99	0.45	0.56	0.74	0.79	1.07	1.00	0.99
Lowest order augmented fully-mixed scheme with adaptive refinement according to $\widetilde{\boldsymbol{\Theta}}$														
466	136.2	-	3.2e-5	-	2.2e-4	-	130.1	-	17.2	-	48.1	-	1.14	
1762	77.45	0.84	2.1e-5	0.58	2.1e-4	0.10	91.72	0.52	0.73	1.28	18.0	1.47	1.09	
6014	56.68	0.50	9.8e-6	1.29	1.5e-4	0.52	65.41	0.55	3.02	1.44	7.04	1.53	1.05	
13206	42.06	0.75	4.1e-6	2.20	8.5e-5	1.58	48.19	0.77	1.61	1.59	3.35	1.88	1.02	
24044	25.83	1.62	2.2e-6	2.10	4.0e-5	2.47	37.02	0.88	0.98	1.64	1.74	2.17	1.00	
48542	13.32	1.88	1.4e-6	1.25	1.9e-5	2.12	26.99	0.89	0.57	1.51	0.81	2.17	1.00	
127678	6.484	1.49	1.0e-6	0.68	9.4e-6	1.47	16.97	0.95	0.31	1.25	0.33	1.81	1.00	
423282	3.190	1.18	6.3e-7	0.78	4.6e-6	1.16	9.344	0.99	0.16	1.09	0.14	1.41	1.00	
Lowest order augmented fully-mixed scheme with adaptive refinement according to $\widehat{\boldsymbol{\Theta}}$														
466	136.2	-	3.2e-5	-	2.2e-4	-	130.1	-	17.2	-	48.1	-		1.11
1762	77.45	0.84	2.1e-5	0.58	2.1e-4	0.11	91.72	0.52	7.34	1.28	18.0	1.47		1.08
6708	56.68	0.46	9.8e-6	1.19	1.5e-4	0.48	65.41	0.50	3.02	1.32	7.04	1.40		1.05
14956	42.06	0.74	4.1e-6	2.18	8.5e-5	1.55	48.19	0.76	1.61	1.56	3.35	1.85		1.02
26122	25.83	1.74	2.1e-6	2.34	4.0e-5	2.66	37.02	0.94	0.98	1.76	1.74	2.34		1.00
52180	13.32	1.91	1.3e-6	1.37	1.9e-5	2.15	26.99	0.91	0.57	1.53	0.81	2.20		0.99
128846	6.484	1.59	9.1e-7	0.83	9.3e-6	1.58	16.97	1.02	0.31	1.33	0.33	1.94		0.99
431240	3.190	1.17	6.3e-7	0.60	4.6e-6	1.14	9.344	0.98	0.16	1.09	0.14	1.40		0.99

Table 5.4: Example 2: Degrees of freedom, individual absolute errors, rates of convergence, and effectivity indexes for the lowest-order augmented fully-mixed finite element method.

[10] I. Babuška and G.N. Gatica, *A residual based a posteriori error estimator for the Stokes-Darcy coupled problem*. SIAM J. Numer. Anal. 48 (2010), no. 2, 498–523.

[11] T.P. Barrios, G.N. Gatica, M. González, and N. Heuer, *A residual based a posteriori error estimator for an augmented mixed finite element method in linear elasticity*. ESAIM Math. Model. Numer. Anal. 40 (2006), no. 5, 843–869.

[12] C. Carstensen, *A posteriori error estimate for the mixed finite element*. Math. Comp. 66 (1997), no. 218, 465–476.

[13] C. Carstensen and G. Dolzman, *A posteriori error estimates for mixed FEM in elasticity*. Numer. Math. 81 (1998), no. 2, 187–209.

[14] C. Carstensen, O. Scherf, and P. Wriggers, *Adaptive finite element for elastic bodies in contact*. SIAM J. Sci. Comput. 20 (1999), no. 5, 1605–1626.

[15] S. Caucao, G.N. Gatica, and R. Oyarzúa, *A posteriori error analysis of an augmented fully mixed formulation for the non-isothermal Oldroyd-Stokes problem*. Numer. Methods PDEs. 35 (2019), no. 1, 295–324.

[16] L. Chen, J. Hu, X. Huang, and H. Man, *Residual-based a posteriori error estimates for symmetric conforming mixed finite elements for linear elasticity problem*. Sci. China Math. 61 (2018), no. 6, 973–992.

[17] C. Cherubini, S. Filippi, A. Gizzi, and R. Ruiz-Baier, *A note on stress-driven anisotropic diffusion and its role in active deformable media*. J. Theoret. Biol. 430 (2017), no. 7, 221–228.

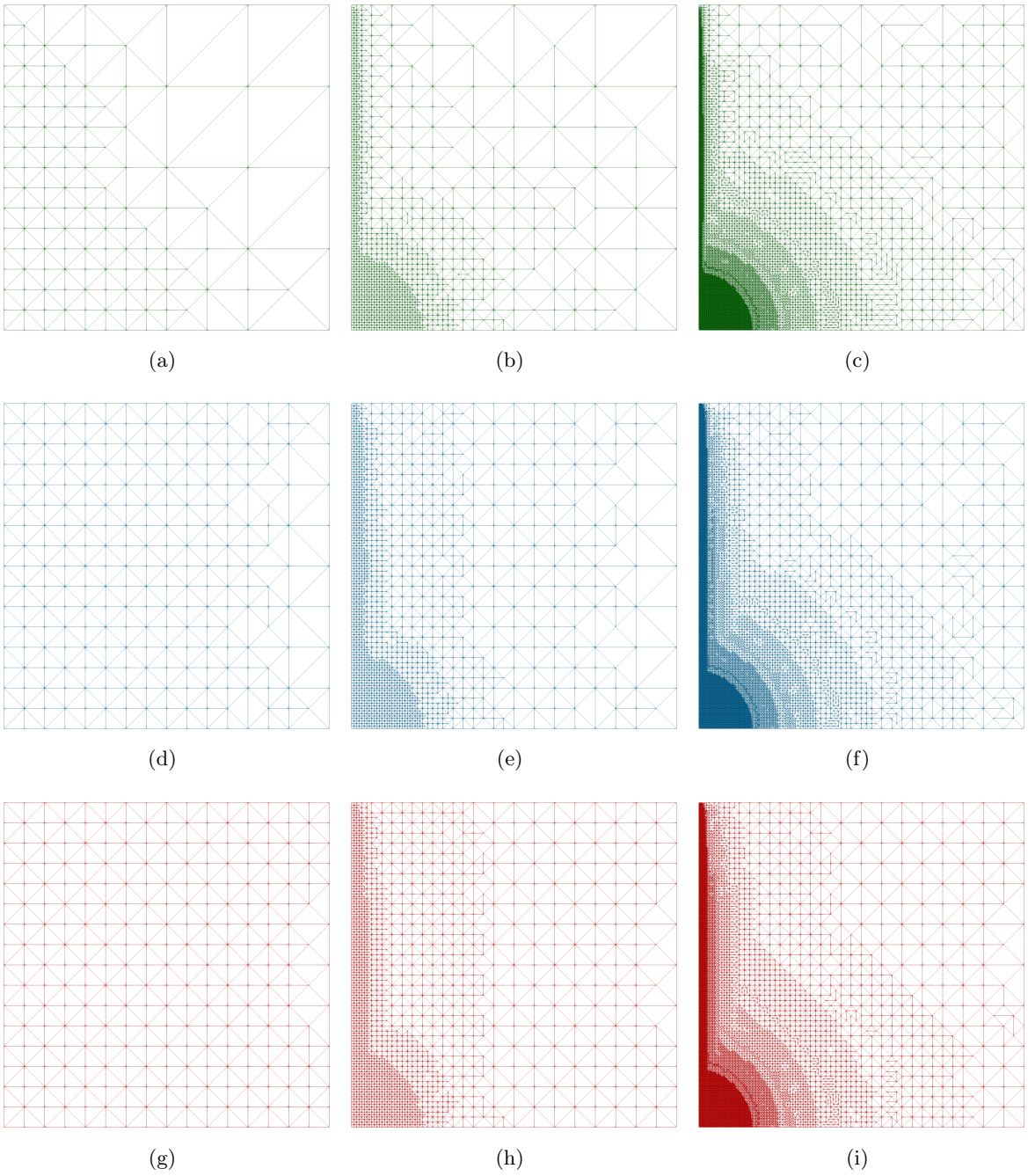

Fig. 5.2: Example 2: From left to right, three snapshots of successively refined meshes according to the indicators $\boldsymbol{\Theta}$ (a,b,c), $\widetilde{\boldsymbol{\Theta}}$ (d,e,f), and $\widehat{\boldsymbol{\Theta}}$ (g,h,i).

[18] P. Ciarlet, *The Finite Element Method for Elliptic Problems*. North-Holland, Amsterdam, New York, Oxford, 1978.

[19] P. Clément, *Approximation by finite element functions using local regularisation*. RAIRO Anal. Numér. 9 (1975), no. R–2, 77–84.

[20] R.W. Cox, *Stress-assisted diffusion: A free boundary problem*. SIAM J. Appl. Math. 51 (1991), no. 6, 1522–1537.

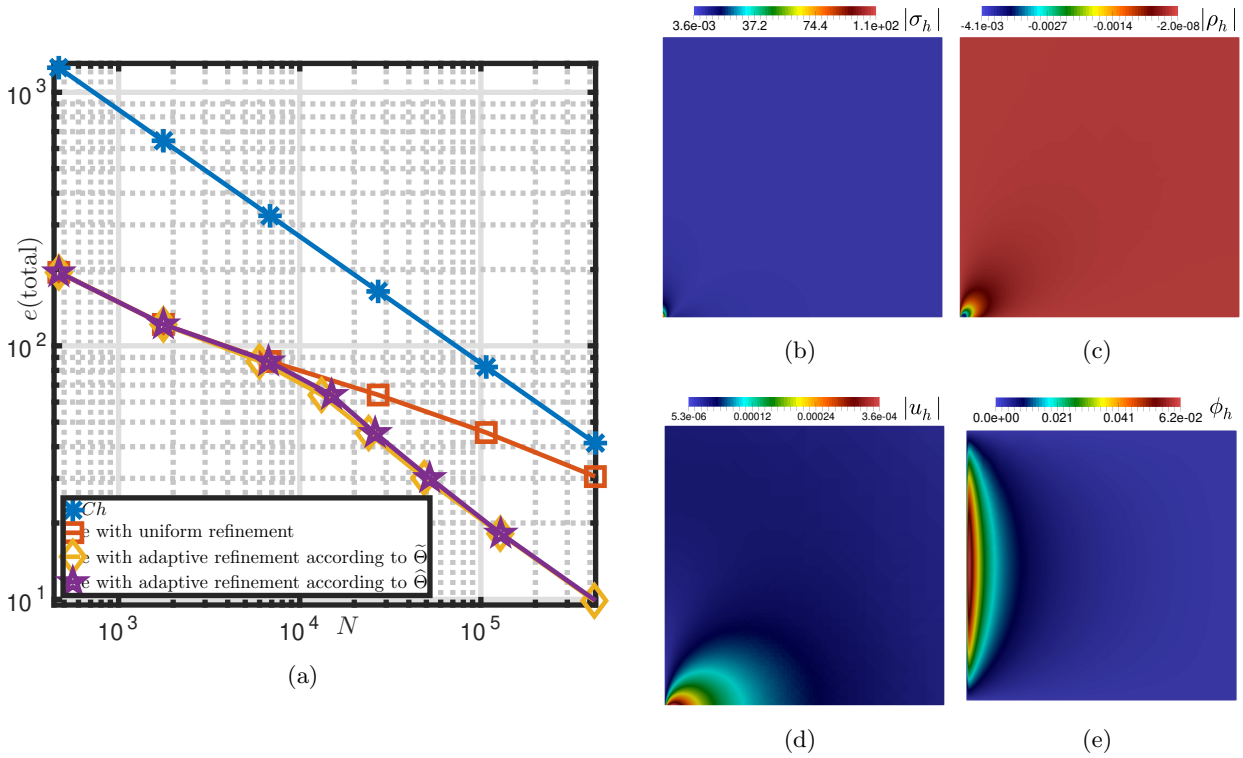

Fig. 5.3: Example 2: Plot of the total error *versus* the number of degrees of freedom N associated with the uniform mesh refinement and adaptive algorithms according to $\widetilde{\boldsymbol{\Theta}}$ and $\widehat{\boldsymbol{\Theta}}$ (a); and approximate stress magnitude (b), rotation magnitude (c), displacement magnitude (d), and solute concentration (e) computed using the lowest-order scheme where mesh adaptation is done via the estimator $\boldsymbol{\Theta}$ after eight steps of refinement.

[21] C. Domínguez, G.N. Gatica, and A. Márquez, *A residual-based a posteriori error estimator for the plane elasticity problem with pure traction boundary conditions*. J. Comput. Appl. Math. 292 (2016), 486–504.

[22] A. Ern and J.-L. Guermond, *Theory and Practice of Finite Elements*. Applied Mathematical Sciences. Springer-Verlag, 2004.

[23] G.N. Gatica, *A Simple Introduction to the Mixed Finite Element Method: Theory and Applications*. Springer Briefs in Mathematics. Springer, Cham 2014.

[24] G.N. Gatica, L.F Gatica, and F.A. Sequeira, *A priori and a posteriori error analyses of a pseudostress-based formulation for linear elasticity*. Comput. Math. Appl. 71 (2016), no. 2, 585–614.

[25] G.N. Gatica, B. Gómez-Vargas, and R. Ruiz-Baier, *Analysis and mixed-primal finite element discretisations for stress-assisted diffusion problems*. Comput. Methods Appl. Mech. Engrg. 337 (2018), 411–438.

[26] G.N. Gatica, B. Gómez-Vargas, and R. Ruiz-Baier, *Formulation and analysis of fully-mixed methods for stress-assisted diffusion problems*. Comput. Math. Appl. 77 (2019), no. 5, 1312–1330.

[27] G.N. Gatica, R. Ruiz-Baier, and G. Tierra, *A posteriori error analysis of an augmented mixed method for the Navier-Stokes equations with nonlinear viscosity*. Comput. Math. Appl. 72 (2016), no. 9, 2289–2310.

[28] A. Khan, C.E. Powell, and D.J. Silvester, *Robust a posteriori error estimators for mixed approximation of nearly incompressible elasticity*. Int. J. Numer. Methods Fluids. 119 (2019), no. 1, 18–37.

[29] M. Lewicka and P.B. Mucha, *A local and global well-posedness results for the general stress-assisted diffusion systems*. J. Elasticity 123 (2016), no. 1, 19–41.

[30] M. Lonsing and R. Verfürth, *A posteriori error estimators for mixed finite element methods in linear elasticity*. Numer. Math. 97 (2004), no. 4, 757–778.

[31] C. Lovadina and R. Stenberg, *Energy norm a posteriori error estimates for mixed finite element methods*. Math. Comp. 256 (2006), no. 75, 1659–1674.

[32] S. Roy, K. Vengadassalam, Y. Wang, S. Park, and K.M. Liechti, *Characterization and modeling of strain assisted diffusion in an epoxy adhesive layer*. Int. J. Solids Struct. 43 (2006), 27–52.

[33] V. Taralova, O. Iliev, and Y. Efendiev, *Derivation and numerical validation of a homogenized isothermal Li-ion battery model*. J. Engr. Math. 101 (2016), 1–27.

[34] J. Toribio and V. Kharin, *Role of Cyclic Pre-Loading in Hydrogen Assisted Cracking*. Environmentally Assisted Cracking: Predictive Methods for Risk Assessment and Evaluation of Materials, Equipment, and Structures. ASTM STP 1401. ASTM, West Conshohocken (PA) (2000), 329–342.

[35] J. Toribio and V. Kharin, *Role of fatigue crack closure stresses in hydrogen assisted cracking*. Advances in Fatigue Crack Closure Measurement and Analysis, ASTM STP 1343, R.C. McClung, J.C. Newman, Eds., ASTM International, West Gonshohocken (1999), 440–458.

[36] C. Truesdell, *Mechanical basis of diffusion*. J. Chem. Phys. 37 (1962), 2336–2344.

[37] R. Verfürth, *A posteriori error estimation and adaptive-mesh-refinement techniques*. J. Comput. Appl. Math. 50 (1994), no. 1-3, 67–83.

[38] R. Verfürth, *A Review of A Posteriori Error Estimation and Adaptive Mesh-Refinement Techniques*. Wiley-Teubner, Chichester, 1996.

[39] R. Verfürth, *A review of a posteriori error estimation techniques for elasticity problems*. Comput. Methods Appl. Mech. Engrg. 176 (1999), 419–440.

[40] T.P. Wihler, *Locking-free adaptive discontinuous Galerkin FEM for linear elasticity problem*. Math. Comp. 75 (2006), no. 255, 1087–1102.

[41] F.G. Yost, D.E. Amos, and A.D. Roming Jr, *Stress-driven diffusive voiding of aluminum conductor lines*. Proc. Int. Rel. Phys. Symp. (1989), 193–201.